ALMA MATER STUDIORUM - UNIVERSITA' DI BOLOGNA
CAMPUS DI CESENA
SCUOLA DI INGEGNERIA E ARCHITETTURA
CORSO DI LAUREA MAGISTRALE IN
INGEGNERIA ELETTRONICA E TELECOMUNICAZIONI
PER LO SVILUPPO SOSTENIBILE

CODED SLOTTED ALOHA WITH MULTIPACKET RECEPTION OVER BLOCK FADING CHANNELS (FOR SATELLITE NETWORKS)

Tesi in: TEORIA DELL' INFORMAZIONE E CODICI LM

Relatore:

Chiar.mo Prof. Ing. Marco Chiani

Presentata da:

Iacopo Mambelli

Correlatori:

Dott. Ing. Federico Clazzer

Dott. Ing. Gianluigi Liva

Dott. Ing. Enrico Paolini

Sessione III
Anno Accedemico 2013-2014

Contents

List of Figures

List of Tables

Introduction

Recently, a lot of devices are supposed to share a common medium, and in this case, different scenarios can be considered, such for example wireless networks, satellite communications, machine to machine communications, system for positioning and so on. Then, protocols that consist to guarantees optimal performance for solve the problem on the Medium Access Control (MAC), without the presence of a central node are required.

Random Access (RA) schemes have been widely studied in the last years, and recently new schemes have been developed. RA schemes represent the best solution to access a common medium which is shared by a large number of users, especially when the users send information sporadically in time (i.e. signalling information). These protocols have low complexity, and due to also their capacity to achieve low transmissions delays, are very appealing. For these reasons, RA schemes are widely used in a satellite communications.

Recent schemes have been developed, called Contention Resolution Diversity Slotted ALOHA (CRDSA), Irregular Repetition Slotted ALOHA (IRSA) and Coded Slotted ALOHA (CSA). These protocols relies on the transmissions of multiple replicas of each data packet and on the Interference Cancellation (IC) technique at the receiver. In particular, the specific techniques used is called Successive Interference Cancellation (SIC).

The main goal of this thesis is to analyze the asymptotic performance of the IC process for IRSA, referred to channels under fading. This can be done, applied the bipartite graph concept at the IC process [21].

The analysis of the IC process in literature has been explained only under collision channel hypothesis. Take into account fading effects is very important, because it is very likely in a real environment that the transmitted signals reach the receiver with different power levels, also due to

fading conditions.

With this first analysis, is possible to find the best polynomial distribution for IRSA (or else the probability to transmits a certain number of replica), fixed the fading conditions. This guarantees to obtain the best throughput achievable by the system.

After the asymptotic analysis, we have compared the obtained results with a finite number of slot for frame. This is the practical case, where the performance degradation with respect to the asymptotic results are shown.

The thesis is organized as follows. In Chapter 1 a brief review of the RA protocols is described. In Chapter 2 we have described the system. Precisely, the chosen fading model and the *Block fading channel* assumption have been explained. Moreover, the users capacity to correctly decode more collided packets in the same slot, also called *capture effect* has been illustrated. This capacity will depend by the considered decoding threshold. In Chapter 3 a brief description on how the threshold can be chose has been considered. In this analysis we have considered only two possible practical case of interest, the first with absence of coding, and the second assuming ideal coding (Shannon limit). In Chapter 4 we have introduced the concept of *Matrix of probability* for representing the capacity of the receiver to correctly decode the packets. We have introduced a mathematical analysis considering the different probabilities as geometrical space regions. The obtained results have been compared with the numerical simulations and the difference in probability terms considering the also presence of SIC. An extension to this model has been found for the probability to correctly decode none of the packets into a certain slot. This one, is needed for the IC analysis of IRSA under fading.

In Chapter 5 we have introduced the IRSA protocol. For first, a recall of the asymptotic analysis of the IC process done with bipartite graphs under collision channel has been done. After that, the asymptotic derivation for the fading channel has been obtained. In particular, the novel scheme that has been introduced, can be applied to a general fading model. Depending on the fading, the description of the probability to correctly decode none of the packets into a certain slot is the only thing that will change. Our model, has also the characteristics to described the probability just mentioned by

a closed formula. So, the relation among this probability and the fading characteristics can be easy analyzed.

Moreover, a theoretical bound has been shown, and some good distributions fixed the fading conditions have been achieved, using a genetic algorithm [27].

In Chapter 6 an introduction to our simulator and the results for IRSA with finite MAC frames, under fading channel, have been shown. Several simulation conditions have been considered, such as for example different frame lengths, different number of SIC iterations, different fading parameters and so on.

At the end the conclusion chapter is presented, where a summary of the achieved results and some ideas about possible future work have been suggested.

Chapter 1

Review of Random Access protocols

RA protocols can be used in packet broadcasting systems where multiple transmitters have to share a common medium. This kind of protocols are used to solve problems as low access delay and also where low complexity of the transmitters and flexibility of the networks are required.

In literature is commonly assumed the so called collision channel hypothesis, in order to derive insightful and simple analytical results. In this case, each packet is correctly received if and only if it does not overlap with others packets sent by the users sharing the network.

The simplest possible solution for such schemes is to let the users transmit packets each time they are ready for transmission, regardless the channel occupation. When a collision it occurs, the users wait a random time and after which it tries a retransmissions of the packet. This could be a good solution when the number of users is quite low and their duty cycle is also limited. When the number of the users increases, the number of packets lost due to collisions increases too. The delays associated at the successful decoding the packet when a collision occurs will be depending by how many times the packet needs to be retransmitted and how long the users must be wait until the retransmission.

The first RA wireless networks, called ALOHA System [1], was implemented at the University of Hawaii where the goal of the project was to interconnect several terminals of the university sites with the wireless

connections.

In the ALOHA System, the throughput can be defined as the mean number of the packets that are correctly received during a certain time τ that represents the time duration of the packet. We define the traffic G as the number of mean packets that the users want sending into the channel into the same time τ. If the traffic is generated from an infinite population of users and it follows a Poisson process, is possible to define the throughput as [1]:

$$S = Ge^{-2G}, [pk/\tau]$$

In the hypothesis that all the transmitted packets have the same duration, for avoiding a collisions at the receiver is needed that no user sends a packet τ second before and after the start of a given packet.

In order to derive the traffic at which the peak throughput is achieved, we use the condition of

$$\frac{\mathrm{d}}{\mathrm{d}G}S = 0 \tag{1.1}$$

$$\frac{\mathrm{d}}{\mathrm{d}G}Ge^{-2G} = 0 \longrightarrow e^{-2G} + G(-2)e^{-2G} = 0 \longrightarrow e^{-2G} = 2Ge^{-2G} \longrightarrow G = \frac{1}{2}$$

So the peak throughput is located at $G = 0.5$ and the peak's value is 0.18 as we can compute and plotting it in Figure 1.1. This protocol has a low throughput and the max efficiency of 18%, then is very low. In fact for avoiding collisions it is necessary that no one transmits in the interval of 2τ. A possible solution that overcomes this issues came with the introduction of Slotted ALOHA. Here, there is a central clock that establishes a sequence of temporal "slots" where the packets can be transmitted. Upon the generation of a packet from higher layers, the packet transmission will start only at the beginning of the next slot, slightly increasing the transmission delay w.r.t ALOHA. Each slot has a duration equal to the duration of a packet, and, if there are collisions, the collision is total among the transmitted packets.

This technique increases the transmitter complexity due to the presence of common clock but on the other hand it has also an advantage in

throughput performance. In fact now, for avoiding the collisions it is necessary that no users transmit in the interval of τ instead of 2τ, this consists in an increase of the throughput.

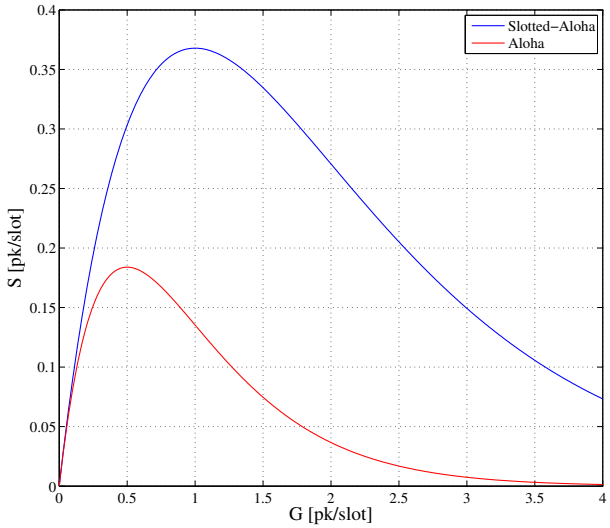

Figure 1.1: Throughput ALOHA and Slotted ALOHA protocols.

Also in this case we can demonstrate what is the traffic value that corresponds to the peak of throughput. From equation (1.1) and taking into account the probability to have no collisions in τ seconds (e^{-G}) we can say:

$$\frac{\mathrm{d}}{\mathrm{d}G}Ge^{-G} = 0 \longrightarrow e^{-G} + G(-1)e^{-G} = 0 \longrightarrow e^{-G} = Ge^{-G} \longrightarrow G = 1$$

So the peak of throughput is 0.36 [pk/slot], double with respect to ALOHA.

A generalization of the SA in which the users send more copies of the same packet in a different frequency channel (frequency diversity) or in a different time slot (time diversity) is also called Diversity Slotted ALOHA (DSA), [3]. When a packet is ready to be sent, k copies of the same packet are transmitted. More precisely, after the first copy, the user waits a random reschedule time for transmitting the second copy and so on, until all the copies are transmitted. The user waits a certain time before it transmits the packet because it is possible to consider each copy

independent by the successive. If the transmitter does not receive the acknowledge from any of those replicas (at least one), it will wait another time the random time and will restart with the transmission procedure. The description just mentioned is referred at the case with *Probabilistic Packet Transmission*, or else where each of the k copies are sending with probability one. It is also possible to consider the case in which each of the k transmission can happen with a certain probability, but it is possible to show that the deterministic policy is always better than the probabilistic policy [3].

If the traffic follows a Poisson process, it is possible to see in [3] that the performance of DSA are sightly better than the SA case, for low offered traffic. The improvement of the performance is minor, at the expense of an higher traffic load injected into the network.

After these, have been developed different protocols which the main goal was to improve the throughput performance and the packets transmissions delay over a wide range of traffic offered. This it means to find some protocols which have the relation between S and the offered traffic linear over an higher interval of G respect the SA and DSA protocols.

The most important of them is called CRDSA [4]. This one is a simple but effective improvement of the Slotted ALOHA System, more precisely is possible to consider it as an improve of the DSA scheme with the adoption of IC techniques [5]-[8], for resolve the collisions. The presence of the IC technique is the real innovation, fundamental for trying to resolve the collision into the MAC frame. Each user transmits two replicas of the same packet (also called $burst$) in a randomly chosen slots, into the same MAC frame, where this one is composed by N_{slot} slots. Each replica has a pointer, which indicates all the slot occupied by the bursts. Whenever one packet is successfully decoded at the receiver, the pointer is extracted and the potential interference contribution caused by the replica on the corresponding slot is removed, such as in the slot where the packet is decoded. The IC technique (precisely the SIC) proceeds until either all bursts have been successfully decoded or until a maximum number of iterations has been reached. This technique is fundamental for improving the performance of the protocol but at the same time introduces a temporal delay proportional to the maximum number of iterations done by the receiver.

The CRDSA protocol achieves a throughput peak close to 0.55 [pk/slot], obtaining a remarkable gain respect to the throughput of Slotted ALOHA.

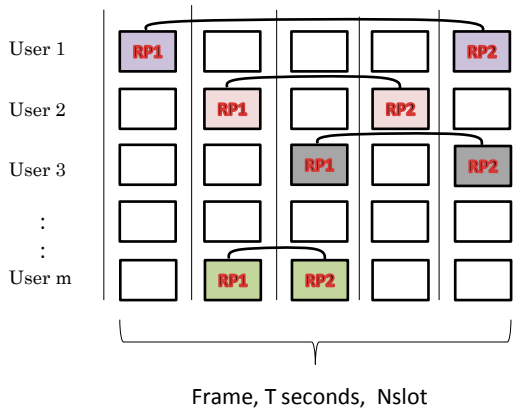

Figure 1.2: Example of a possible CRDSA MAC frame. T is the time of the MAC frame defined as $N_{slot}T_s$ where T_s is the time corresponding to each time slot and where N_{slot} represents the number of slots composing the MAC frame.

RA protocols described until now are widely used in satellite networks both to share a common medium, both when the transmission of short packets is required. Some applications are for example the Digital Video Broadcasting Return Channel via Satellite (DVB-RCS) [9] and IP over Satellite (IPoS) standard [10].

When instead, is required the transmission of longer packets or the users want to offering a medium to high level of traffic into the satellite networks will use for example the Demand Assignment Multiple Access protocol (DAMA), [11], [12] and [13].

DAMA protocol consists to achieve a throughput gain than the RA protocols, especially when a medium to high traffic is offered. Each user has a dedicate resources in which it can transmits. The resources are allocated

by a central node and the simplest method to reserve the use of the channel is by request of the users. However this protocol suffers of long delays, especially when the round-trip time is high like in the satellite networks. Then during the creation of the establishing connection are still preferred the RA protocols.

Chapter 2

Collision and Block Fading Channel Models

The collision channel hypothesis is assumed in all the RA papers (such as CRDSA, IRSA and so on) because it consists to abstract the physical layer and permits to analyze the MAC layer independently, so is more easy to analyze it.

The collision channel model assumes that the packets involved in a collision are completely lost. There are many practical cases where this assumption can be pessimistic because also in presence of collisions is possible to correctly decode one or more packets. In fact, especially in a mobile communication scenarios, it is very likely that one of the signals dominates the others so the packets reach the receiver with different powers and the so-called *capture effect* can arise. In generally, that happens because the packets are subjected to different antenna gains, to different characteristics of the transmitter terminals, to different locations with respects to the receiver, to different fading conditions and so on. Fading accounts for random fluctuations of power due to the characteristic of propagations's environment as, for example, the presence of multipath (the received signal is constituted by different paths of the transmitted signal, where each of this paths is associated to a certain delay and to a certain attenuation, due to the reflections) and as, for example, at the relative motion among the transmitter and receiver, which causes time variations of the channel. Thanks to the fading effects, the idea that packets involved in collisions

can be successfully decoded is born and this capacity of the decoder is called *capture effect*. Clearly this capacity will depend on the channel conditions, higher the difference of power is among the received packets and more probable the strongest packet can be correctly decoded.

The multiple paths can cause time dispersions and frequency selectivity. These paths are present both in a mobile telecommunications environment in which the fluctuations of power are described with statistical properties and also in a fixed telecommunications system where in this case the fluctuations of power can be described in deterministic mode, because the users do not move.

The presence of multiple paths is measured in the frequency domain by the coherence bandwidth of the channel (B_c), which represents the frequency separation at which two frequencies components of the signal undergo independent attenuation. The reciprocal of B_c is the multipath spread which is the delay associated to the last received path of the transmitted signal. For avoid the distortion phenomenon we have to obey to $B < B_c$, i.e. the bandwidth of the transmitted signal must be less than B_c, or else the time duration of the transmitted symbol greater than the delay associated at the last path, otherwise we have a frequency selective fading.

So, the multipath phenomenon will depend on the time duration of the transmitted signal in the environment in which it will propagate.

With one example I will show how is possible to describe what is the behavior of multiple paths. Precisely the example that I will describe is referred to determinist fading, situation of practical interest. The example considers a fixed number of propagation paths (two paths) where their characteristic can be defined individually. This case represents the situations in which the transmitter and the receiver are fixed and only two paths of propagation are considered. This could be as an example, the simplest version of a terrestrial radio channel.

The received signal can be written as:

$$y(t) = x(t) + \upsilon x(t - \tau)$$

where υ and τ indicates respectively the amplitude of the second path (will be an attenuation) and the delay associated (in other words we have assumed that the first path has no attenuation).

If we assume the channel linear and time-invariant, its transfer function will be:

$$H(f) = 1 + \upsilon e^{-\jmath 2\pi f \tau}$$

in which the terms υ, $e^{-\jmath 2\pi f \tau}$ describe the multipath component (associated at the second path), so it has magnitude described as:

$$\begin{aligned} \mid H(f) \mid &= \sqrt{(1 + \upsilon \cos(2\pi f \tau))^2 + \upsilon^2 \sin^2 2\pi f \tau} \\ &= \sqrt{1 + \upsilon^2 + 2\upsilon \cos(2\pi f \tau)} \end{aligned}$$

By the expression just wrote is possible to see that depending on the product ($f\tau$), the transfer function introduces a gain or an attenuation, so it depends on the delays.

If the transmitter and the receiver are in relative motion, the parameters υ and τ become time-variant and the transfer function of the channel will depend also on time. One parameter that it takes into account the relative motion among the transmitter and the receiver is called *Doppler effect*. This effect is a frequency shift of the received signal proportional to the relative speed and to the carrier frequency. The doppler effect, in conjunction with multipath propagation, can cause frequency dispersion and time selective fading. These phenomena make the power associated at the received signal is aleatory, precisely the random variables that describe the received power will be an amplitude and phase factor. In a digital transmission, the fading effect hits the received signal introducing a variation of its in terms of amplitude and phase respect the transmitted signal. When is possible to consider the fading effect constant during the time in which the signal goes from the transmitter to the receiver, it has not time-variant characteristics, then it is so called *Slowly Fading*, otherwise is called *Fast fading*.

In our case we will focus only on the slowly fading channel case, because this one can be well represents the Satellite communications scenario. Moreover we have assumed that the parameters of fading can be considered constant not only for the received symbol but for an entire packet. This is the *Block-Fading channel* assumption in which we say that

the $R.V.$ of the envelope and phase associated to the received symbols, are constant for all symbols belongings to the same packet.

In the case of *Block-Fading channel* the received signal is described as:

$$r_{ri} = \alpha\, e^{\jmath\phi} s_{ti} + z_i \tag{2.1}$$

where $(i = 0, 1, \ldots, l-1)$ and l is the number of symbols inside the packet.

The transmitted signal s_t arrives at the receiver attenuated by α, and with a phase shift ϕ.

There are several fading model that reflect the behavior of many realistic channels. In our case we have decided to consider the fading as a Rayleigh distributed for which the random variable associated at this distribution is:

$$X = \sqrt{X_1^2 + X_2^2}, \quad \mathbb{E}[X] = \sigma_1 \sqrt{\frac{\pi}{2}}$$

where X_1 and X_2 are normally distributed according with variance σ_1^2. Its possible to demonstrate that the Rayleigh variable is the square root of random variable χ^2 with two degrees of freedom [14]. Moreover the χ^2 with two degrees of freedom is also an exponential random variable. We can conclude that the Rayleigh variable is the square root of the exponential random variables. Therefore the power is exponentially distributed, as:

$$f_x(x) = \begin{cases} \frac{1}{P_m} e^{-\frac{x}{P_m}} & \text{for } x > 0 \\ 0 & \text{otherwise} \end{cases} \tag{2.2}$$

Where P_m is mean value of the distribution. So the parameter α in the equation (2.1) will be described as a Rayleigh distributed.

By equation (2.2), is possible to see that the power follows a negative exponential, where the delay to zero will depend on the mean of the distribution. The phase variations are due to propagation delays of the transmitted signal. It is reasonable to think that this *R.V.* is $\mathcal{U}$(-π,π). For having a complete model, we have to take into account the thermal noise of the channel (z), which is a *R.V.*$\sim\mathcal{N}(0, \sigma_n^2)$ where σ_n^2 is the noise variance.

When the receiver is able to 'capture' more than one packet in the same time slot, we are talking about *Multi Packet Reception Capability*, due for example to at the different powers with which the packets are received.

Considering the fading aspects we are able to introduce a more realistic physical layer.

How can is possible to decide if the packet is correctly received (and then correctly decoded) or not? It depends on the level of interfering and noise power that the considered signal suffers. It is possible to establish a maximum value of interfering power for which we are able to decode the packet. This can be done, exploiting the definition of the Signal to Interference Noise Ratio (SINR). The $SINR_i$ represents the power associated at the received packet i respect the interferes (also the noise). When we have a total of n transmitted packets into a certain slot, is:

$$\gamma_i = \frac{P_i}{N + \sum_{\substack{k=1 \\ k \neq i}}^{n} P_k} = \frac{\Gamma_i}{1 + \sum_{\substack{k=1 \\ k \neq i}}^{n} \Gamma_k} \tag{2.3}$$

where P_i represents the power with which the i-th packet is received, N is the noise power and where $\Gamma_i = P_i/N$ is the Signal to Noise Ratio (SNR).

The reference signal shall be stronger than the interference signal. How much stronger depends on the threshold considered. The threshold, represents the minimum value of SINR necessary to correctly decode a received packet. In general the threshold depends on the set of modulation and coding scheme that has been selected for the link, by the packet error rate target and by the packet length. In the next chapter we will briefly discussed how is possible to chose the threshold value.

Chapter 3

Threshold Based Decoding

The threshold value b represents the minimum SINR for which we consider the packet correctly decoded. We will focus on determining the threshold in two cases of practical interest:

1. Absence of the coding;
2. Assuming ideal coding (*Shannon Bound*);

3.1 Absence of coding

Every telecommunication system has a maximum percent of lost packet that can be accepted, depending on the application. We can define this quantity as a Packet Error Rate (PER) target , so the system must be realize at least for guarantee this value of PER.

Each packet consists of a certain number bits N_b. We can define the BER as the probability that a received bit is not correct and we can denote it with p_b. There is a simple relation for a system that does not use coding between the PER and BER, this it depends on the packet length. We will see later that know the BER and the modulation scheme used, it permits to find the minimum SINR for decoding a packet, i.e. b the threshold.

Defined P_s as the probability of correctly receiving a packet, in the absence of coding, P_s coincides with the probability of receiving all bits correctly, so

$$P_s = (1 - p_b)^{N_b}$$

So the PER will be:

$$\text{PER} = 1 - P_s = 1 - (1 - p_b)^{N_b}$$

We can seen from the Figure 3.1 that the points simulated for high BER follow perfect the theoretical curve, while for low BER does not happen. The reason is because we do not have enough simulation rounds for each point for generating a good statistics. In order to increase the precision, we would need to simulate more points.

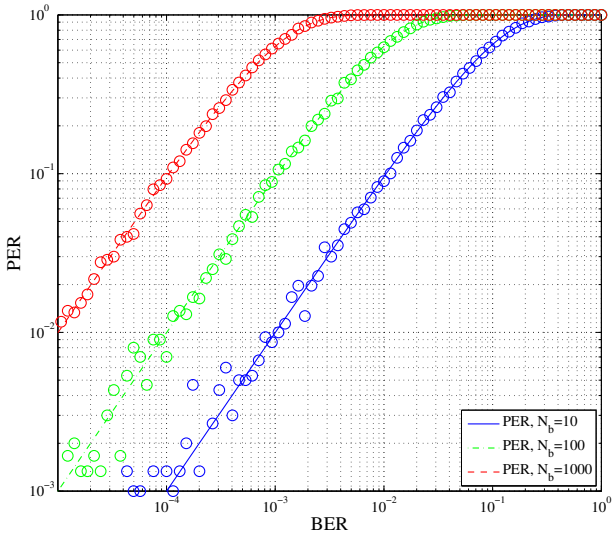

Figure 3.1: Comparison between the theoretical PER and the simulated PER for different packet lengths N_b. The number of simulation is fixed equal to 3000 for each BER value.

By the system at which we referred, in the case of absence of coding, is possible to find the corresponding BER by the requested PER and packet length value.

For obtaining the value of the threshold we need for guaranteeing the target PER, we must understand how the choice of the modulation impact the target PER, and therefore BER. In Figures 3.2, 3.3 and 3.4 different *Symbol error rate* curves are drawn, where the *Symbol error rate* represents

the probability of not correctly received a symbol, versus the E_s/N_0. The Symbol error rate is a function of E_s/N_0 and of the modulation scheme selected. For drawing these curves of Symbol error rate, I have used as a reference the theoretical formulas in [14].

A generic transmitted symbol is constituted by $\log_2 M$ bits where M is the modulation index, so we can write the *Symbol Error Rate* as the $\log_2(M)p_b$, in the hypothesis that we used the Grey code.

We can observe that, fixed Symbol Error Rate, the value of minimum E_s/N_0 changes with the modulation scheme that is used.

In Figure 3.4 I have drawn the *Symbol error rate* versus the E_s/N_0 for a Gaussian Minimum Shift King (GMSK) modulation. This modulation uses two symbols, so the *Symbol error rate* and the E_s/N_0 can be represents at the same time by the BER and E_b/N_0 respectively, where E_b/N_0 represents the bit signal to noise ratio. Moreover, this curve is obtained with the hypothesis of absence of Fading . In this case the BER is [18]:

$$p_b = \frac{1}{2} erfc \sqrt{\alpha \frac{E_b}{N_0}} \tag{3.1}$$

where α represents a constant value of attenuation and where the $erfc$ is represented by the well-known function

$$erfc(x) = \frac{2}{\sqrt{\pi}} \int_0^x e^{-t^2} dt$$

Equation (3.1) is obtained as the BER of antipodal scheme, with a supplementary attenuation, because choosing the time bandwidth product of the premodulation gaussian filter $B_bT = 0.25$, the performance degrades of the GMSK than the antipodal scheme can be approximate by the α factor.

It is clear now how the threshold can be founded in absence of coding. In fact from the PER request and the packet length we are able to achieve the corresponding BER. The value just found with the modulation scheme used permits to find the corresponding *Symbol error rate*, and by this one, for the fixed modulation schemed, the minimum E_s/N_0 that satisfied the specific request is founded. For example, if we fixed $(1 - P_S) = 10^{-3}$, $N_b = 100$ and the modulation schemes as 16-QAM, we satisfy the specific for $E_s/N_0 \geq 19.76$ so $b = 19.76$ in this case.

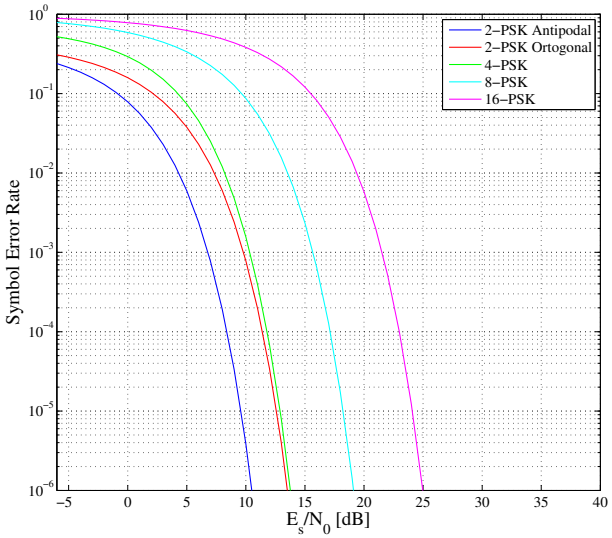

Figure 3.2: M-PSK vs E_s/N_0.

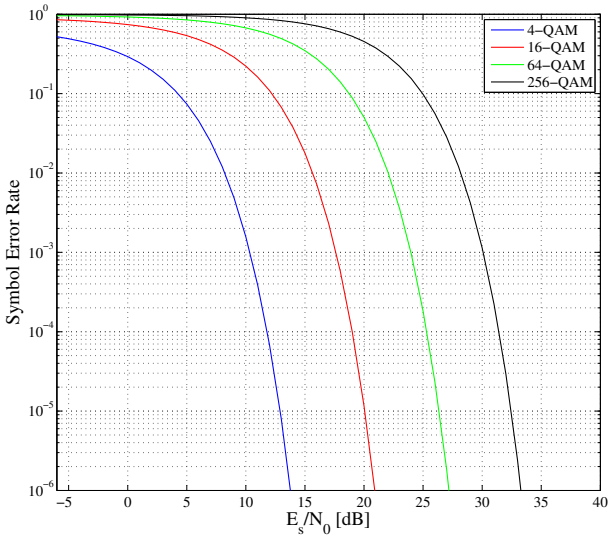

Figure 3.3: M-QAM vs E_s/N_0.

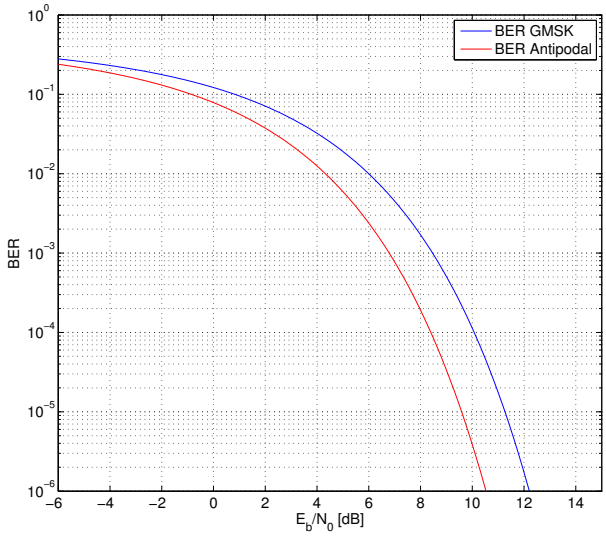

Figure 3.4: GMSK vs E_b/N_0 with $B_bT = 0.25$, where B_bT represents the time bandwidth product.

3.2 Ideal codify of *Shannon*

Shannon defines the Capacity of the channel as a maximum value of the $Rate$ ($bit/s/Hz$ or bit for channel use, transmitted into the channel) with which is possible to obtained vanishing probability of error of the transmitted signal at the decoder. For a gaussian channel is possible to define the capacity C as:

$$C = \log_2(1 + E_b/N_0)\ [bit/s/Hz] \tag{3.2}$$

Where C is normalized to the bandwidth B and where E_b/N_0 is the bit signal to noise ratio.

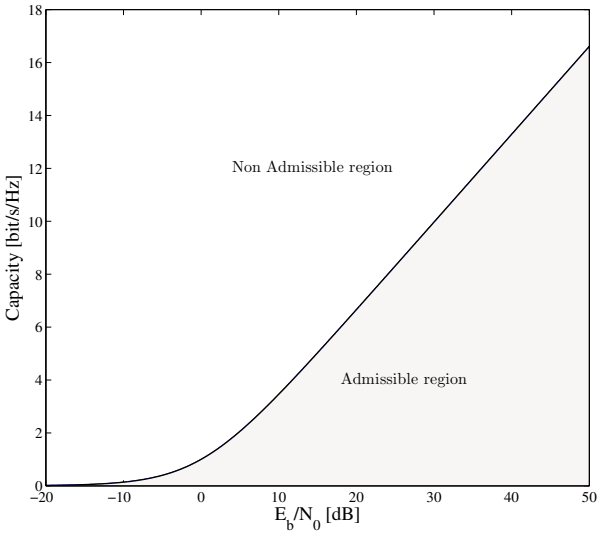

Figure 3.5: Shannon limit vs E_b/N_0

Shannon only tells us that this is possible, not how we can achieve this limit. For example with a certain code or methods, but only that is possible to achieve a very low error probability if we use $R \leq C$, where R is the Rate.

As we can see from the equation (3.2), the capacity is a function of the E_b/N_0, precisely it easily showed that the capacity is directly proportional to the log of E_b/N_0.

We can write the capacity given of equation (3.2) also as:

$$C = B \log_2 \left(1 + \frac{E_b R_s}{N_0 B}\right) \ [bit/s] \tag{3.3}$$

Where R_s represents the transmission Rate into the channel in $bit/second$. With this definition of capacity is possible to show [15] that for a gaussian channel with an unlimited bandwidth we have an inferior limit to the signal to noise ratio request for every kind of telecommunication systems that want to transmit with low probability of error. This limit is:

$$E_b/N_0 \geq -1.59 \ [dB]$$

If we assume that the channel is instead limited in bandwidth we define the spectral efficiency ξ, that is depending from the type of code and modulation scheme that we used as:

$$\xi = \frac{R_s}{B} \ [bit/s/Hz]$$

which determinates a lower bound of the signal to noise ratio. We can demonstrate [15], that over an Additive White Gaussian Noise (AWGN) channel with spectral efficiency, every system requires a minimum signal to noise ratio for guaranteeing low error probability:

$$E_b/N_0 \geq \frac{2^{\xi} - 1}{\xi}$$

This describes in the plane $E_b/N_0, \xi$ one permitted region and one region that is not permitted.

In the systems where the fundamental resource is the bandwidth, we are looking to have high spectral efficiency, where the high efficiency is achievable with high signal to noise ratio (at the expanse of the battery life of who transmits). Instead, in the systems where the fundamental resource is E_b/N_0, we are looking to have very low signal to noise ratio, so at the expanse of the spectral efficiency.

If we use a set of modulation and scheme of coding, we can define the total Rate as:

$$R_s = \ R_c \cdot log_2(M)$$

where R_c is the coding Rate, whereas R_m is the Rate of the modulation.

If this Rate (R_s) is less or equal to the capacity, we can have a reliable transmission. Otherwise, we cannot guarantee reliable communication.

If the encoder associates one output bit to one input bit, R_c will be 1 and the capacity will be depending only from the $log_2\ M$, where M is the modulation index.

Under this hypothesis, we have evaluated the performance of the different modulation schemes versus the Shannon limit, where E_s/N_0 represents as usual the symbol signal to noise ratio.

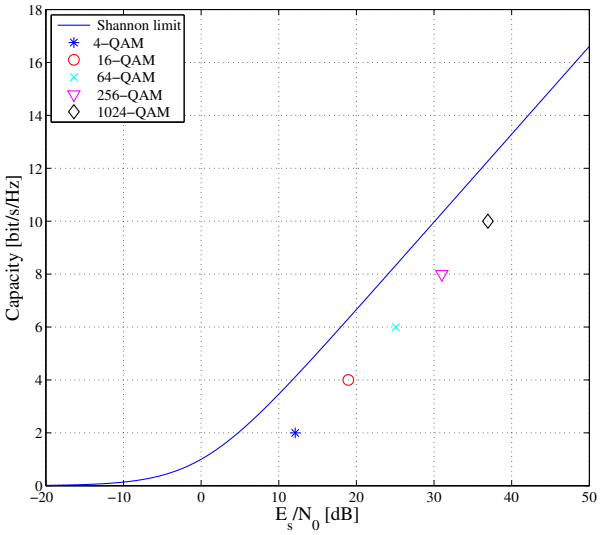

Figure 3.6: M-QAM vs Shannon limit. The chosen packet error rate is 10^{-2} and $N_b = 184$.

We selected both the target PER andthe packet length based on the Automatic Identification System (AIS), [16]. The target PER is 10^{-2}, and the number of bits chosen for packets is 184, where the information occupies 168 bits and there are 16 bits of Cyclic Redundancy Check (CRC), used for checking if the packet has been corrupted.

In the AIS packet there are a total of 256 bits, but the remaining ones except for the 184 are associated to the training sequence, to the start flag and to the end flag. These sections of the packet are used for synchronization purpose at the receiver and for indicating the start of the data.

Since these packet sections are fixed, we can assume that, achieved the frame sync, errors may occur only in the data or CRC fields of the packets.

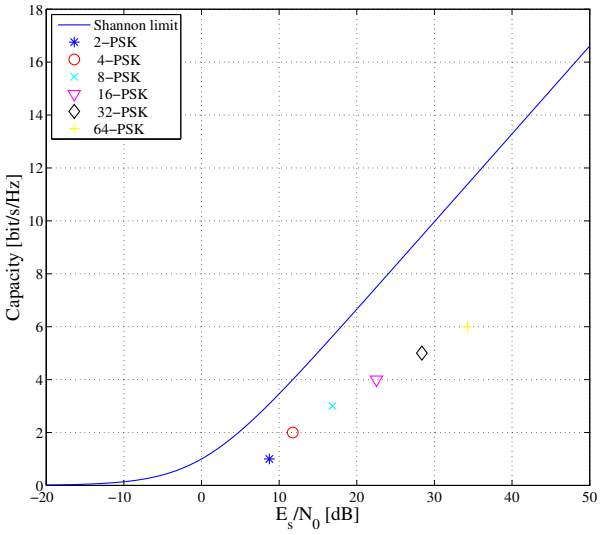

Figure 3.7: M-PSK vs Shannon limit. The chosen packet error rate is 10^{-2} and $N_b = 184$.

We can make the following observations looking at Figure 3.8, that:

- For low E_s/N_0 is more convenient the use of the modulation with low data rate. Otherwise, if we chose a modulation with very high data-rate, we cannot obtain a low probability of error. Instead, when we have high value of signal to noise ratio, is more convenient to increase the modulation order, for having a higher spectral efficiency, so we can exploit the good conditions of the channel.
- If we compare the 2-PSK with the GMSK modulation, we can see that the use of the GMSK is worst in terms of E_s/N_0 (a bit) but it is possible with this modulation to keep control of the envelope of the transmitted signal, making the spectrum of the output power more compact.
- If we do not use coding, although we are in absence of fading, we are far from the Shannon limit.

If we use the Shannon limit for determine the minimum value of E_s/N_0 that we have need for having a correct reception of the information, we find:

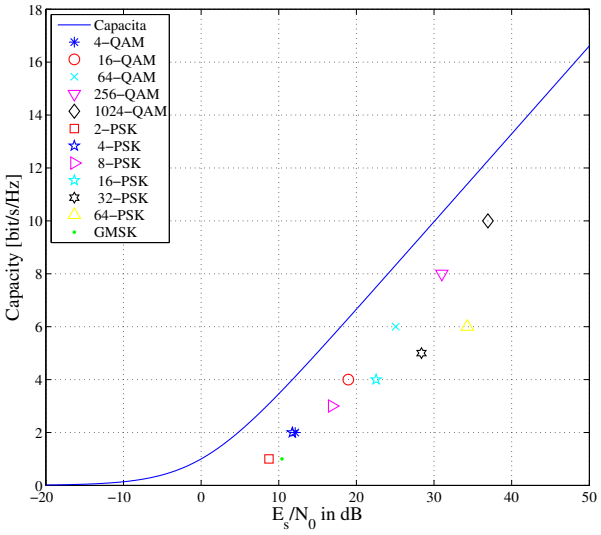

Figure 3.8: All the modulation vs Shannon limit. The chosen packet error rate is 10^{-2} and $N_b = 184$.

$$C = R_s = \log_2(1 + E_s/N_0) \longrightarrow 2^{R_s} = (1 + E_s/N_0)$$
$$\Longrightarrow b = (2^{R_s} - 1)$$

Then, the value just found b represents the minimum signal to interference noise ration which allows a correctly decoded of the packet. In this case our threshold model is a step function because we have assumed that each packet is correctly received if the correspond SINR is greater equal than b.

In reality, the Shannon limit is not achievable also with the application of existent code (for guarantee low probability of error) so the request value of E_s/N_0 will be greater with respect to the one that we have found.

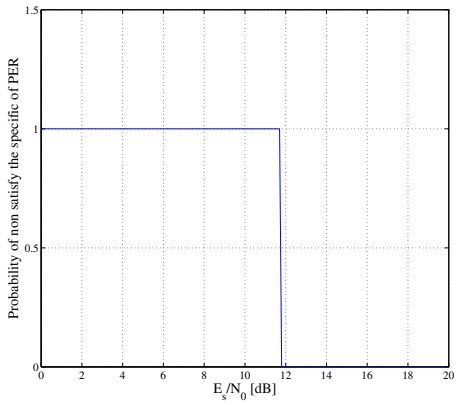

Figure 3.9: Threshold level that we have assumed in this caption, where if the E_s/N_0 is greater equal at the threshold, it follows the correctly decoded of the packet. We have chosen the $R_s = 4$.

Chapter 4

Matrix of Probability in case of *Multi-Packet Reception*

The scope of this chapter will be to describe the probability matrix M_p, characterized by a specific fading model; precisely the fading will be Rayleigh distributed. The M_p matrix has been introduced for first in [17], and it represents the capacity of the receiver to receive more than one packet in the same time slot. Each coefficient of this matrix will be represent the probability to correctly decoded a packet when a certain number of packet are collided into the slot. This matrix concepts can be applied in all cases where the multi packet reception capability is considered, for example in RA protocols in both slotted and unslotted system, considering both the presence of SIC and not.

Is possible to define its as:

$$M_p = \begin{pmatrix} R_{1,0} & R_{1,1} & 0 & \dots & & \\ R_{2,0} & R_{2,1} & R_{2,2} & 0 & \dots & \\ R_{3,0} & R_{3,1} & R_{3,2} & R_{3,3} & 0 & \dots \\ \vdots & \vdots & \vdots & \vdots & \ddots & \end{pmatrix}$$

where the generic coefficient $R_{n,k}$ represents the probability to corrected decoding k packets when n have been sent. If we consider two packets that are collided, then we consider the second row of the matrix M_p. In this case, we can evaluate the different terms of probability that we achieve with and without the contribute of IC. Specifically, we will make the as-

sumption of threshold decoding. If SIC is employed, the receiver tries to decode for first the packet with the highest SINR and if the decoding is successfully, its contribution is removed. The procedure can be repeated many times (iterative mode) and its depends on the power contribution of the packets collided, from the threshold and from the noise.

If we consider two packets collided, the coefficients of the M_p Matrix can be described as:

$$R_{2,0} = Prob\left\{\frac{P_1}{N+P_2} < b \;\; and \;\; \frac{P_2}{N+P_1} < b\right\} \tag{4.1}$$

This expression represents the probability that none of the packets can be decoded, where P_1 and P_2 are the received power of the two packets whereas b represents the threshold and N is the noise power. The formula (4.1) is valid both with SIC and without it. Instead, if the system does not have the capacity of removing the interference, we can determine $R_{2,1}$, $R_{2,2}$ as:

$$\begin{aligned} R_{2,1} = Prob\Bigg\{&\left(\frac{P_1}{N+P_2} \geq b \;\; and \;\; \frac{P_2}{N+P_1} < b\right) \\ &or \;\; \left(\frac{P_2}{N+P_1} \geq b \;\; and \;\; \frac{P_1}{N+P_2} < b\right)\Bigg\} \end{aligned}$$

$$R_{2,2} = Prob\left\{\frac{P_1}{N+P_2} \geq b \;\; and \;\; \frac{P_2}{N+P_1} \geq b\right\} \tag{4.2}$$

On the other hand, when the system can erase the contribution of the interference we can determine the same coefficient as:

$$\begin{aligned} R_{2,1} = Prob\Bigg\{&\left(\frac{P_1}{N+P_2} \geq b \;\; and \;\; \frac{P_2}{N} < b\right) \\ &or \;\; \left(\frac{P_2}{N+P_1} \geq b \;\; and \;\; \frac{P_1}{N} < b\right)\Bigg\} \end{aligned}$$

$$R_{2,2} = Prob\left\{\left(\frac{P_1}{N+P_2} \geq b \ \ and \ \ \frac{P_2}{N} \geq b\right) \right.$$
$$\left. or \ \ \left(\frac{P_2}{N+P_1} \geq b \ \ and \ \ \frac{P_1}{N} \geq b\right)\right\}$$

The other terms of the second matrix's row, are different as we can see from the formulas above written. As a result I expected an increase of the probability to correctly decoded both the packets due to the SIC.

Drawing the curves of SINR as a function of the powers we can identify different regions, where each of these represents a certain coefficient of the matrix M_p. We focus for first at the $n = 2$ case, considering a threshold $b \geq 1$.

4.1 Matrix elements's M_p for $n = 2$ and $b \geq 1$

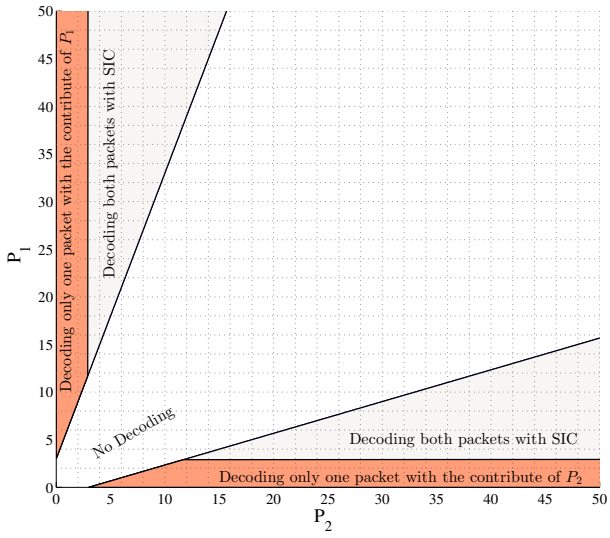

Figure 4.1: Plot of the probability's regions for $n = 2$ and $b = 3$.

Its possible to evaluate the row of the M_p matrix with the following methods:

The area corresponding to $R_{2,0}$ is delimited by two curves, that are function of P_1 and P_2. We have assumed that P_1 and P_2 have the same

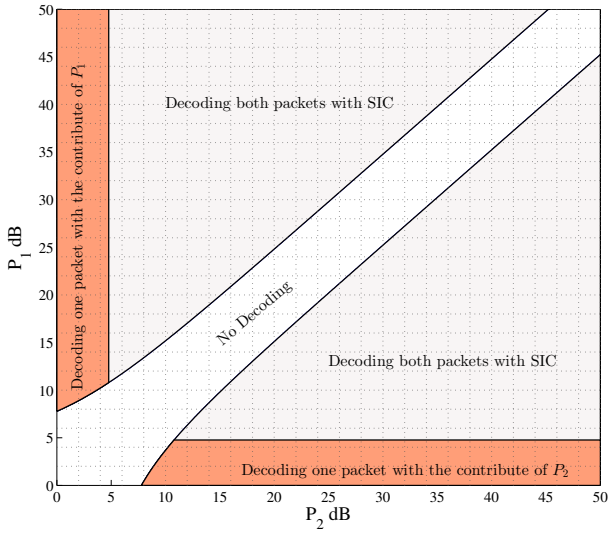

Figure 4.2: Plot of the probability's regions for $n = 2$ and $b = 3$, with P_1 and P_2 in logaritmic domain.

distributions and the same mean value P_m (equation (2.2)), so that is possible to divide the area into two symmetric regions, with the bisector of P_1 and P_2. If we integrated the area between the bisector and the curve $Nb + P_2 b$ and multiplied this by two, we are able to know the value of $R_{2,0}$.

$$
\begin{aligned}
R_{2,0} &= 2\int_0^{\infty}\int_{P_2}^{Nb+P_2b} \frac{1}{P_m^2} e^{-\frac{(P_1+P_2)}{P_m}}\, dP_1\, dP_2 \\
&= 2\int_0^{\infty} \frac{1}{P_m^2} P_m \left[-e^{-\frac{(P_1+P_2)}{P_m}}\right]_{P_2}^{Nb+P_2b} dP_2 \\
&= 2\int_0^{\infty} \frac{1}{P_m} \left(-e^{-\frac{(Nb+P_2b+P_2)}{P_m}} + e^{-\frac{(2P_2)}{P_m}}\right) dP_2 \\
&= 2\frac{1}{P_m}\int_0^{\infty} -e^{-\frac{(Nb+P_2b+P_2)}{P_m}}\, dP_2 + 2\frac{1}{P_m}\int_0^{\infty} e^{-\frac{2P_2}{P_m}}\, dP_2 \\
&= \frac{2}{(b+1)}\left[e^{\frac{-(Nb+P_2(b+1))}{P_m}}\right]_0^{\infty} - \left[e^{-\frac{2P_2}{P_m}}\right]_0^{\infty} \\
&= 1 - \frac{2e^{-\frac{Nb}{P_m}}}{(b+1)}
\end{aligned}
$$

where $\frac{1}{P_m^2} e^{-\frac{(P_1+P_2)}{P_m}}$ represents the pdf conditioned at the value of P_1 and

P_2. With a similar argument, it is also possible to determine the value of $R_{2,1}$ e $R_{2,2}$.

$$\begin{aligned}
R_{2,1} &= 2\int_0^{Nb}\int_{Nb+P_2b}^{\infty}\frac{1}{P_m^2}e^{-\frac{(P_1+P_2)}{P_m}}\,dP_1\,dP_2 \\
&= 2\int_0^{Nb}\frac{1}{P_m}\left[-e^{-\frac{(P_1+P_2)}{P_m}}\right]_{Nb+P_2b}^{\infty}dP_2 \\
&= 2\int_0^{Nb}\frac{1}{P_m}e^{-\frac{(Nb+P_2b+P_2)}{P_m}}\,dP_2 \\
&= 2\frac{e^{-\frac{Nb}{P_m}}}{(b+1)}\left[-e^{-\frac{P_2(b+1)}{P_m}}\right]_0^{Nb} \\
&= 2\frac{e^{-\frac{Nb}{P_m}}}{(b+1)}\left(1-e^{-\frac{Nb(b+1)}{P_m}}\right)
\end{aligned}$$

$$\begin{aligned}
R_{2,2} &= 2\int_{Nb}^{\infty}\int_{Nb+P_2b}^{\infty}\frac{1}{P_m^2}e^{-\frac{(P_1+P_2)}{P_m}}\,dP_1\,dP_2 \\
&= 2\int_{Nb}^{\infty}\frac{1}{P_m}\left[-e^{-\frac{(P_1+P_2)}{P_m}}\right]_{Nb+P_2b}^{\infty}dP_2 \\
&= 2\int_{Nb}^{\infty}\frac{1}{P_m}e^{-\frac{(Nb+P_2b+P_2)}{P_m}}\,dP_2 \\
&= \frac{2}{(b+1)}\left[-e^{-\frac{(Nb+P_2(b+1))}{P_m}}\right]_{Nb}^{\infty} \\
&= \frac{2}{(b+1)}e^{-\frac{(Nb+Nb(b+1))}{P_m}} \\
&= \frac{2}{(b+1)}e^{-\frac{Nb(b+2)}{P_m}}
\end{aligned}$$

The next step is compares the coefficient terms derived analytically versus the integral of the probability density function of these regions obtained numerically.

I have written a MATLAB script that can be used to simulate the collision among two packets. A Monte Carlo simulation with 10^6 rounds, $b = 3$

and $P_m = 10$ has been chosen. We can see this in Table 4.1, where the almost perfect match between the results confirm the analytical derivation.

	$R_{2,0}$	$R_{2,1}$	$R_{2,2}$
analytic	0.629	0.258	0.111
simulation	0.630	0.259	0.110

Table 4.1: Probability values of M_p matrix calculated by analytical way and simulation results, for $n = 2$ and $b \geq 1$.

4.2 Matrix elements's M_p for $n = 2$ and $b < 1$

The case of $b < 1$ determines that the curves (function of P_1 and P_2, $Nb + P_2b, Nb + P_1b$) intersect each other in a certain point which depends from the value of b. In this way we have a certain region that is in common between the curves. This region represents the values of P_1 and P_2 where we can correctly decode the packets in absence of SIC. The Figure 4.3 shows this case.

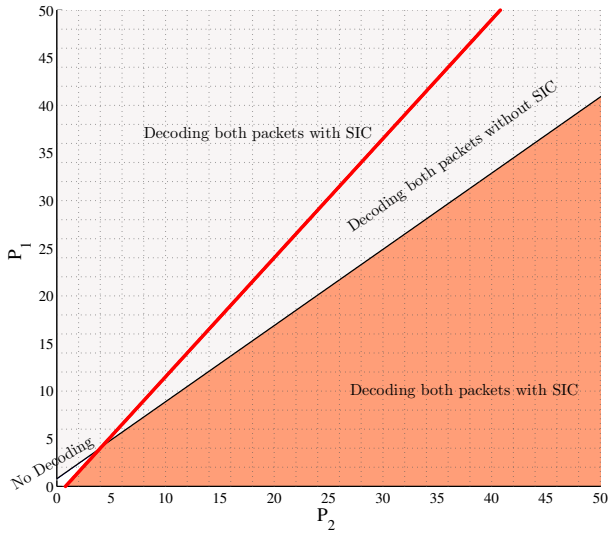

Figure 4.3: Graph with the regions with negative threshold.

- As we can see from the figure above, the region in which is not possible to correctly decode, tightens to the origin of the axis, becoming smaller. The more the value of b is decreasing, more this area will be tighten to the origin;
- The regions where is possible to correctly decode one packet will become infinitesimal;
- From the intersecting point of the curves, we have an area in which is possible to correctly decode both the packets without SIC;
- The presence of the SIC allows to correctly decode both packets in the other regions.

Also in this case, we have compared the analytical value with the integral of the probability density function of these regions. It can be observed that in the region which is possible to correctly decode only one packet, they do not intersect. So the analytical formulas used in the case $b \geq 1$ are still valid except for the $R_{2,2}$ term. In this case the analytical evaluation of this term it can be represented by the formula:

$$\begin{aligned} R_{2,2} = &\int_{Nb}^{\infty} \int_{Nb+P_2b}^{\infty} \frac{1}{P_m^2} e^{-\frac{(P_1+P_2)}{P_m}} \, dP_1 \, dP_2 + A_t \\ &+ \int_{x'}^{\infty} \int_{Nb}^{Nb+P_2b} \frac{1}{P_m^2} e^{-\frac{(P_1+P_2)}{P_m}} \, dP_1 \, dP_2 \end{aligned}$$

where x' represents the intersection point of the curves in the x axis whereas A_t represents the area of the triangle that is outside the calculation of the integrals. So:

$$\begin{aligned} R_{2,2} = &\overbrace{\int_{Nb}^{\infty} \frac{1}{P_m} e^{-\frac{(Nb+P_2b+P_2)}{P_m}} \, dP_2 + A_t}^{A_1} \\ &+ \underbrace{\int_{x'}^{\infty} \frac{1}{P_m} \left(-e^{-\frac{(Nb+P_2b+P_2)}{P_m}} + e^{-\frac{(Nb+P_2)}{P_m}} \right) dP_2}_{A_2} \end{aligned}$$

The sum of the first terms of the integral can be expressed like this:

$$A_1 = \int_{Nb}^{\infty} \frac{1}{P_m} e^{-\frac{(Nb+P_2b+P_2)}{P_m}} \, dP_2 + A_t \quad = \frac{1}{P_m} e^{-\frac{Nb}{P_m}} \int_{Nb}^{\infty} \left(e^{\frac{-P_2(b+1)}{P_m}} \right) dP_2 + A_t$$

$$A_1 = \frac{e^{-\frac{Nb}{P_m}}}{(b+1)} \left[-e^{\frac{-P_2(b+1)}{P_m}} \right]_{Nb}^{\infty} + A_t$$

$$A_1 = \frac{e^{-\frac{Nb}{P_m}}}{(b+1)} \left(e^{\frac{-Nb(b+1)}{P_m}} \right) + A_t$$

the other term instead:

$$A_2 = \int_{x'}^{\infty} \frac{1}{P_m} \left(-e^{-\frac{(Nb+P_2b+P_2)}{P_m}} + e^{-\frac{(Nb+P_2)}{P_m}} \right) dP_2$$

$$A_2 = \int_{x'}^{\infty} \frac{1}{P_m} \left(-e^{-\frac{(Nb+P_2b+P_2)}{P_m}} \right) dP_2 + \int_{x'}^{\infty} \frac{1}{P_m} \left(e^{-\frac{(Nb+P_2)}{P_m}} \right) dP_2$$

$$A_2 = \frac{1}{(b+1)} \left[e^{-\frac{(Nb+P_2b+P_2)}{P_m}} \right]_{x'}^{\infty} - \left[e^{-\frac{(Nb+P_2)}{P_m}} \right]_{x'}^{\infty}$$

so finally:

$$R_{2,2} = A_1 + A_2 = e^{-\frac{Nb}{P_m}} \left(\frac{-e^{\frac{-(x'(b+1))}{P_m}}}{(b+1)} + e^{-\frac{x'}{P_m}} \right)$$

In this case we have determined the term of $R_{2,0}$ as a difference from the others terms because in this case is not easy to extract it in an analytical way. We can compare again the analytical value with the simulation probability derived from the Monte Carlo simulation about the collided packets. This result is shown in Table 4.2.

	$R_{2,0}$	$R_{2,1}$	$R_{2,2}$
analytical	0.025	0.137	0.838
simulation	0.024	0.137	0.839

Table 4.2: Probability values of M_p matrix calculated by analytical way and simulation way, for $n = 2$ and $b < 1$.

For the simulation we have chosen $N_{sim} = 10^6$, $b = 0.8$ and $P_m = 10$.

4.3 Matrix elements's M_p for $n = 3$ and $b \geq 1$

After the case with two collisions, we move to the third row of the matrix M_p. We consider for the moment the presence of SIC with $b \geq 1$. We supposed that the collided packets have the same distribution of power, following the Rayleigh distribution for the envelope of the signal and we suppose also that we are able to order at the receiver the packets with a decreasing level of power. We generally indicate their decreasing SINR as $\gamma_1 \geq \gamma_2 \geq \gamma_3$. In this situations is possible to determine $R_{3,2}$ and $R_{3,3}$ as:

$$
\begin{aligned}
R_{3,2} &= Prob\left\{\left(SNIR_1 \geq b \quad and \quad \frac{P_2}{(N+P_3)} \geq b \quad and \quad P_3 < Nb\right)\right\} \\
&= Prob\left\{(P_1 \geq Nb + P_2 b + P_3 b \quad and \quad P_2 \geq Nb + P_3 b \quad and \quad P_3 < Nb)\right\} \\
&= 6\int_0^{Nb}\int_{Nb+P_3b}^{\infty}\int_{Nb+P_2b+P_3b}^{\infty} \frac{1}{P_m^3} e^{-\frac{(P_1+P_2+P_3)}{P_m}}\, dP_1\, dP_2\, dP_3 \\
&= 6\int_0^{Nb}\int_{Nb+P_3b}^{\infty} \frac{1}{P_m^2}\left[-e^{-\frac{(P_1+P_2+P_3)}{P_m}}\right]_{Nb+P_2b+P_3b}^{\infty} dP_2\, dP_3 \\
&= 6\int_0^{Nb}\int_{Nb+P_3b}^{\infty} \frac{1}{P_m^2} e^{-\frac{(Nb+P_2b+P_3b+P_2+P_3)}{P_m}}\, dP_2\, dP_3 \\
&= 6\int_0^{Nb}\int_{Nb+P_3b}^{\infty} \frac{1}{P_m^2} e^{-\frac{(Nb+P_2(b+1)+P_3(b+1))}{P_m}}\, dP_2\, dP_3 \\
&= 6\int_0^{Nb} \frac{1}{P_m(b+1)}\left[-e^{-\frac{(Nb+P_2(b+1)+P_3(b+1))}{P_m}}\right]_{Nb+P_3b}^{\infty} dP_3 \\
&= 6\int_0^{Nb} \frac{1}{P_m(b+1)}\left(e^{-\frac{(Nb+(Nb+P_3b)(b+1))+P_3(b+1)}{P_m}}\right) dP_3 \\
&= 6\frac{e^{-\frac{(2Nb+Nb^2)}{P_m}}}{(b+1)}\int_0^{Nb} \frac{1}{P_m} e^{-\frac{(P_3(b+1)^2)}{P_m}}\, dP_3
\end{aligned}
$$

$$= 6\frac{e^{-\frac{(2Nb+Nb^2)}{P_m}}}{(b+1)^3}\left[-e^{-\frac{(P_3(b+1)^2)}{P_m}}\right]_0^{Nb}$$
$$= 6\frac{e^{-\frac{(2Nb+Nb^2)}{P_m}}}{(b+1)^3}\left(1-e^{-\frac{(Nb(b+1)^2)}{P_m}}\right) \tag{4.3}$$

$$\begin{aligned}
R_{3,3} &= Prob\left\{\left(SNIR_1 \geq b \;\; and \;\; \frac{P_2}{(N+P_3)} \geq b \;\; and \;\; P_3 \geq Nb\right)\right\} \\
&= Prob\left\{(P_1 \geq Nb + P_2b + P_3b \;\; and \;\; P_2 \geq Nb + P_3b \;\; and \;\; P_3 \geq Nb)\right\} \\
&= 6\int_{Nb}^{\infty}\int_{Nb+P_3b}^{\infty}\int_{Nb+P_2b+P_3b}^{\infty}\frac{1}{P_m^3}e^{-\frac{(P_1+P_2+P_3)}{P_m}}\,dP_1\,dP_2\,dP_3 \\
&= 6\int_{Nb}^{\infty}\int_{Nb+P_3b}^{\infty}\frac{1}{P_m^2}\left[-e^{-\frac{(P_1+P_2+P_3)}{P_m}}\right]_{Nb+P_2b+P_3b}^{\infty}dP_2\,dP_3 \\
&= 6\int_{Nb}^{\infty}\int_{Nb+P_3b}^{\infty}\frac{1}{P_m^2}e^{-\frac{(Nb+P_2b+P_3b+P_2+P_3)}{P_m}}\,dP_2\,dP_3 \\
&= 6\int_{Nb}^{\infty}\int_{Nb+P_3b}^{\infty}\frac{1}{P_m^2}e^{-\frac{(Nb+P_2(b+1)+P_3(b+1))}{P_m}}\,dP_2\,dP_3 \\
&= 6\int_{Nb}^{\infty}\frac{1}{P_m(b+1)}\left[-e^{-\frac{(Nb+P_2(b+1)+P_3(b+1))}{P_m}}\right]_{Nb+P_3b}^{\infty}dP_3 \\
&= 6\int_{Nb}^{\infty}\frac{1}{P_m(b+1)}\left(e^{-\frac{(Nb+(Nb+P_3b)(b+1))+P_3(b+1)}{P_m}}\right)dP_3 \\
&= 6\frac{e^{-\frac{(2Nb+Nb^2)}{P_m}}}{(b+1)}\int_{Nb}^{\infty}\frac{1}{P_m}e^{-\frac{(P_3(b+1)^2)}{P_m}}\,dP_3 \\
&= 6\frac{e^{-\frac{(2Nb+Nb^2)}{P_m}}}{(b+1)^3}\left[-e^{-\frac{(P_3(b+1)^2)}{P_m}}\right]_{Nb}^{\infty} \\
&= 6\frac{e^{-\frac{(2Nb+Nb^2)}{P_m}}}{(b+1)^3}\left(e^{-\frac{(Nb(b+1)^2)}{P_m}}\right) = 6\frac{e^{-\frac{(3Nb+3Nb^2+Nb^3)}{P_m}}}{(b+1)^3}
\end{aligned} \tag{4.4}$$

Like the previous bidimensional case, in equation (4.3) and equation (4.4), I have put in front of the integrals a multiplying factor for taking into account all the regions in which is possible to correctly decode two packets, this factor is 6.

How is possible to see, the evaluation of the coefficient's Matrix is be-

coming difficult, because increase order of collision, means to increase the spatial dimension that we have to take into account.

4.4 First column of Matrix's probability

For our scope it is sufficient to find the value of the first column of this Matrix, independently if b is greater or not than one.

We assume that each packet is received with a certain power level P_0 which follows a Rayleigh distribution with mean value P_m. Calling P_i the received interfering power (of the i-th interfering user), if we assume that the received powers are i.i.d. by equation (2.2), we can say that:

$$Pr\left\{\frac{P_0}{N+\sum_{i=1}^{n} P_i} < b\right\} = Pr\left\{P_0 < bN + b\sum_{i=1}^{n} P_i\right\}.$$

Recalling equation (2.2) we know that

$$P_0, P_i \sim \begin{cases} \frac{1}{P_m} e^{-\frac{x}{P_m}} & x > 0 \\ 0 & x \leq 0 \end{cases}$$

Then

$$Pr\left\{P_0 < bN + b\sum_{i=1}^{n} P_i\right\} =$$

$$= \int_0^\infty \cdots \int_0^\infty Pr\left\{P_0 < bN + b\sum p_i | P_i = p_i, i = 1, ..., n\right\} \cdot$$

$$\cdot Pr\left\{P_i = p_i, i = 1, ..., n\right\} \prod_{i=1}^{n} dp_i.$$

We know that

$$F(x) = \int_0^x \frac{1}{P_m} e^{-\frac{\xi}{P_m}}\, d\xi = 1 - e^{-\frac{\xi}{P_m}}.$$

So,

$$
\begin{aligned}
&Pr\left\{P_0 < bN + b\sum_{i=1}^{n} P_i\right\} = \\
&= \int_0^\infty \cdots \int_0^\infty \left(1 - e^{-\frac{bN + b\sum p_i}{P_m}}\right) \prod_{i=1}^{n} \frac{1}{P_m} e^{-\frac{p_i}{P_m}} dp_i = \\
&= 1 - e^{-\frac{bN}{P_m}} \left[\prod_{i=1}^{n} \frac{1}{P_m} \int_0^\infty e^{-\frac{b+1}{P_m} p_i} dp_i\right] = \\
&= 1 - e^{-\frac{bN}{P_m}} \left[\frac{b+1}{P_m}\right]^{-n} P_m^{-n} = \\
&= 1 - e^{-\frac{bN}{P_m}} \left[b+1\right]^{-n}
\end{aligned} \tag{4.5}
$$

The equation (4.5), represents then the probability of no decoding a packet when n are collided. The results depends on n, on the threshold b, on the noise power N, and on the mean of the fading distribution.

For notation simplification we indicate $\gamma^* = b$ and $\bar{\Gamma} = \frac{P_m}{N}$, so the equation (4.5) can be also write as:

$$
Pr\left\{P_0 < bN + b\sum_{i=1}^{n} P_i\right\} = 1 - e^{-\frac{\gamma^*}{\bar{\Gamma}}} \left[\gamma^* + 1\right]^{-n} \tag{4.6}
$$

Chapter 5

IRSA

IRSA is a generalization of the CRDSA protocol introduced in Chapter 1. In fact, while CRDSA protocol sends two replicas for each packet, IRSA choses a random number of replicas, from a given probability distribution.

At the receiver the SIC techniques has been employed. It has been shown in [21] and [22] that this kind of techniques can be well modeled by means of a bipartite graph, that is typically used in information theory.

The probability distribution selected will influence the performance of the protocol. The aim will be to find the best distribution for each average number of possible transmitted replicas.

As a first step we introduce the graph representation of the IC process under the collision channel hypothesis, after that we will extend it for Rayleigh fading.

5.1 Graph Representation of the IC Process

In IRSA, each user selected the repetition rate based on a certain probability distribution $\{\Lambda_d\}$. The generic Λ_l represents the probability to transmits l replicas into the MAC frame.

The representation of the MAC frame is depicted in Figure 5.1, where each slot can be represented with a $sum\ node$, each user can be represented with a burst node (circle) and where each user replica is represented by an edge departing from the burst node to a sum node. Both sum nodes and burst nodes have a certain $degree$ that is the number of edges emanat-

ing from this node. We focus on these nodes for explaining how the IC evolves; this approach is also called *Node Perspective Distribution*.

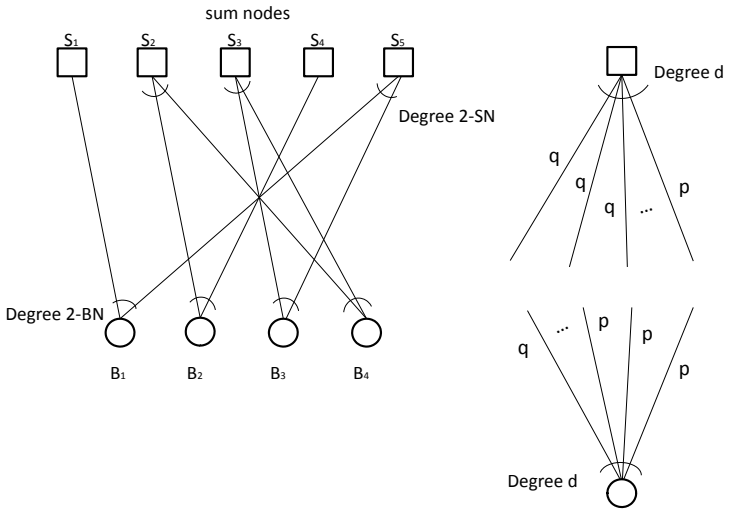

Figure 5.1: Representation of the MAC frame by bipartite graph on the left and the *Node Perspective Distribution* on the right. In this example, both slot node and transmitter node are represented with degree d (right hand side picture).

With the Node Perspective Distribution the burst node and the sum node distribution are described respectively by

$$\Lambda(x) = \sum_l \Lambda_l x^l, \quad \Psi(x) = \sum_l \Psi_l x^l$$

where the generic elements Ψ_l represent the probability that a sum node has l edges and therefore degree l.

It is clear that the burst node distribution $\Lambda(x)$ is under full control of the system designer, while this is not the case for $\Psi(x)$ of the sum nodes. We can also define the average burst rate as $\Lambda'(1) = \sum_l \Lambda_l l$ and the average number of packets for slot as $\Psi'(1) = \sum_l \Psi_l l$.

The degree distribution can be defined also from the *Edges Perspective* where we define λ_l the probability that an edge is connected to a burst node with degree l and ρ_l the probability that the edge is connected at a sum node with degree l. The definitions of these parameters are given by:

$$\lambda_l = \frac{\Lambda_l l}{\Lambda'(1)}, \quad \rho_l = \frac{\Psi_l l}{\Psi'(1)}$$

and the corresponding polynomial distribution are represented by

$$\lambda(x) = \sum_l \lambda_l x^{l-1}, \quad \rho(x) = \sum_l \rho_l x^{l-1}$$

We consider the node perspective of Figure 5.1 where the transmitter and the sum node have degree d.

From the point of view of the burst node the probability q that an edge is unknown, corresponding at the probability that the others replicas has not been corretly decoded in the previous iteration, so

$$q_i = p_{i-1}^{d-1}$$

From the point of view of one sum node in similar mode let us call p the probability that an edge is unknown, given that each of the other $d-1$ edges has been revealed with probability (1-q) in the previous step. Here the edge is revealed whenever all the other edges have been revealed, so

$$p_i = 1 - (1 - q_i)^{d-1}$$

By averaging these two expressions over the edge distributions, one can derive the evolution of the average erasure probabilities as

$$\bar{q_i} = \sum_l \lambda_l \bar{p}_{i-1}^{(l-1)} \tag{5.1}$$

$$\bar{p_i} = \sum_{c=1}^{\infty} \rho_c (1 - (1 - \bar{q_i})^{(c-1)}) \tag{5.2}$$

The offered traffic is generated following a Poisson distribution so ρ_c can be written as:

$$\rho_c = \frac{\bar{G}\Lambda'(1)^{c-1}}{(c-1)!} e^{-\bar{G}\Lambda'(1)} \tag{5.3}$$

where $\bar{G}$ is the mean offered traffic.

5.1.1 IC convergence analysis for collision channel

By iterating equations (5.1), (5.2) it is possible to analyze the convergence of the IC process. Given q_0, p_0 can be evaluated using equation (5.2). As the new p_0 becomes available, q_1 can be also computed using equation (5.1). We can then proceed the iterations until a convergence is found.

We can resume the iterative equation for the collision channel case in briefly as:

$$\begin{cases} q_0 = \bar{q_0} = 1 \\ \bar{p_i} = \sum_{c=1}^{\infty} \rho_c (1 - (1 - \bar{q_i})^{(c-1)}) & i = 0, ..., \infty \\ \bar{q}_{i+1} = \sum_{l} \lambda_l \bar{p_i}^{(l-1)} \end{cases}$$

The accuracy of the equations (5.1) and (5.2), during the iterations, is subject to the absence of loops in the graphs. This assumption implies very large frames sizes ($N_{slot} \to \infty$), so we show in the next the results refer to the asymptotic settings. Its important to underline that this analysis will be also valid for short or moderate-length frames. We will show this by numerical results.

Once $\Lambda(x)$ is fix, it will exist a certain value of offered traffic called G^* under which it is possible to recover the bursts with probability close to one. If the offered traffic is greater than G^* the procedure will fail to recover bursts with a certain probability far from 0.

The probability to recovere the bursts close to one will be obtained if and only if iteration after iteration $\bar{q}_{i+1} < \bar{q}_i$, so that is possible to define the threshold value as the maximum value of G such that:

$$\bar{q}_i > \lambda(1 - \rho(1 - \bar{q}_i)), \quad \forall\, \bar{q} \in (0, 1]. \tag{5.4}$$

This condition is also represented by the fact that q,$p \to 0$ during the iterations.

Under the assumption that the number of possible transmitting users into the MAC frame $m \to \infty$, is possible to demonstrate that equation (5.4) can be also written as:

$$\bar{q} > \lambda(1 - e^{-\bar{q}G\Lambda'(1)}), \quad \forall\, \bar{q} \in (0, 1]. \tag{5.5}$$

where the index i has been omitted for simplicity.

In the asymptotic case ($N_{slot} \to \infty$) the performance for different distribution referred in terms of MAC burst loss probability, P_L (i.e., the probability that the transmission attempt does not succeed) vs the normalized offered traffic can be obtained. The relation between the throughput S and P_L is given by $S(G) = G(1 - P_L(G))$. The burst loss probability has been obtained by iterating (for each value of G) the equation (5.1) and (5.2) in the case of collision channel. The equations are iterated a certain number of times $I_{max} = 1000$ and after that $P_L = \Lambda(\bar{p})$. This is because the probability p of having an edge unknown is given by the probability that all the edges connected at the burst node are not revealed after the I_{max} iterations, so averaging on the burst node distribution we obtain $P_L = \sum_l \Lambda_l \bar{p}^l$.

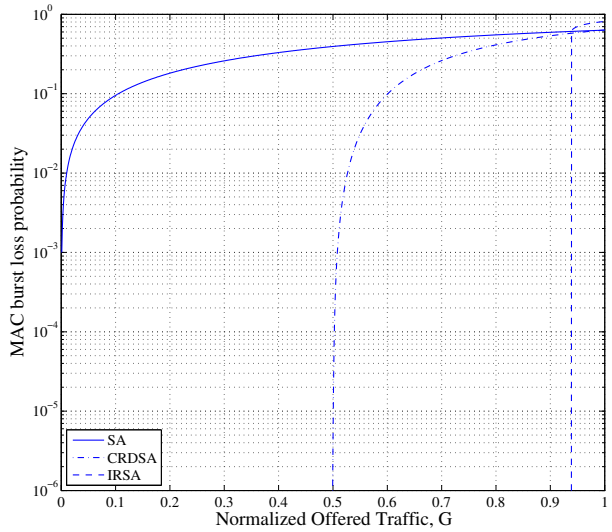

Figure 5.2: Asymptotic performance in terms of MAC packet (burst) loss probability, P_L vs. the offered traffic G, for SA, CRDSA and for IRSA with irregular distribution $\Lambda_1(x) = 0.5x^2 + 0.28x^3 + 0.22x^8$.

In Figure 5.2 we have shown the burst loss probability for SA, CRDSA and IRSA with distribution $\Lambda_1(x) = 0.5x^2 + 0.28x^3 + 0.22x^8$. As we can see from the figure it exists for each distribution a certain value of offered traffic G^* that represents a threshold under which the burst will be recovered

with a probability close to one.

We have resumed in Table 5.1 some different values of G^* obtained for different distributions. The distributions are derived exploiting a genetic algorithm that will be described in section 5.3.5.

Distribution, $\Lambda(x)$	G^*
$0.5102x^2 + 0.4898x^4$	0.868
$0.5631x^2 + 0.0436x^3 + 0.3933x^5$	0.898
$0.5465x^2 + 0.1623x^3 + 0.2912x^6$	0.915
$0.5x^2 + 0.28x^3 + 0.22x^8$	0.938
$0.4977x^2 + 0.2207x^3 + 0.0381x^4 + 0.0756x^5 + 0.0398x^6 + 0.0009x^7 + 0.0088x^8 + 0.0069x^9 + 0.0030x^{11} + 0.0429x^{14} + 0.0081^{15} + 0.0576x^{16}$	0.965

Table 5.1: Thresholds computed for different distributions.

It is clear that in the collision channel the maximum G^* that can be obtaining is $G^* = 1$.

5.2 Generating the Distributions

We are interested in finding for each value of $\Lambda'(1)$ the maximum value of G^* and compare it with a theoretical bound.

For generating the distributions, we have used the truncated soliton distribution (truncated at N terms) [23], [24]. This distributions represents the optimal distribution of the replicas under the assumption of $N_{slot} \rightarrow \infty$. The polynomial representation is expressed as

$$\Lambda^N(x) = \frac{\sum_{l=2}^{N+1} \frac{x^l}{l(l-1)} - \frac{ax^2}{2}}{Q}$$

where Q is a parameter used for normalizing the probability mass function to one, a is one of the parameters distribution such that $a \in (0, 1)$ and N represents the maximum number of replicas that can be transmitted for each packet (the term with which the soliton distribution is truncated).

From $\Lambda^N(x)$ we can obtain the Λ_l of the representation as

$$\Lambda_l = \frac{\Lambda'_l}{Q}$$

where Λ'_l is defined as

$$\begin{cases} \Lambda'_l = \dfrac{1}{l(l-1)} & l > 2 \\ \Lambda'_2 = \dfrac{1}{2(2-1)} - \dfrac{a}{2} = \dfrac{1}{2(1-a)} & l = 2 \end{cases}$$

so the parameter Q used for the normalization will be

$$Q = \sum_{l=2}^{N+1} \frac{1}{l(l-1)} - \frac{a}{2}$$

It is possible to show that if $a \rightarrow 0$ and $N \rightarrow \infty$, the efficiency of the system η, is very close to one, where the efficiency is defined as the number of packets correctly received over the number of slots.

Using the above expression of the polynomial representation $\Lambda^N(x)$ is possible to derive the corresponding $\Lambda'(1)$ (referred at the N truncated terms) as

$$\Lambda'(1) = \frac{H(N) - a}{\sum_{l=2}^{N+1} \frac{1}{l(l-1)} - a}$$

where $H(N)$ represents the Harmonic number, defined as

$$H(N) = \sum_{l=1}^{N} \frac{1}{l}$$

5.2.1 Theoretical bound for the collision channel

For different values of $\Lambda'(1)$ obtained with the soliton distribution, we are able to achieved different values of G^*. These different values can be compared with the theoretical bound [25]. The main idea for explaining how the bound can be evaluated is to draw the functions q and p during the SIC iterations (drawing each in function of the other). We can then show that an open tunnel must be present between the curves as a necessary condition for have a successful decoding of the packets. The condition which guarantees this is given by $A_b + A_s < 1$ where A_b and A_s are respectively the areas of the function $q = f_b(p)$ and $p = f_s(q)$. The areas can be easily calculated, recalling the equations (5.1) and (5.5), as

$$
\begin{aligned}
p = f_s(q) \Rightarrow A_s &= \int_0^1 (1 - e^{-q\bar{G}\Lambda'(1)}) \ dq \\
&= 1 - \left[-\frac{e^{-q\bar{G}\Lambda'(1)}}{\bar{G}\Lambda'(1)} \right]_0^1 \\
&= 1 - \frac{1}{\bar{G}\Lambda'(1)} \left(1 - e^{-\bar{G}\Lambda'(1)} \right)
\end{aligned}
$$

and

$$
q = f_b(p) \Rightarrow A_b = \sum_l \lambda_l \int_0^1 p^{l-1} \ dp = \sum_l \lambda_l \left[\frac{p}{l} \right]_0^1 \Rightarrow
$$

so,

$$
A_b = \frac{1}{\Lambda'(1)}. \tag{5.6}
$$

In this way combining both areas,

$$
\begin{aligned}
&\frac{1}{\Lambda'(1)} + 1 - \frac{1}{\Lambda'(1)\bar{G}} + \frac{e^{-\bar{G}\Lambda'(1)}}{\Lambda'(1)\bar{G}} < 1 \\
&\frac{1}{\Lambda'(1)} < \frac{1}{\Lambda'(1)\bar{G}} \left(1 - e^{-\bar{G}\Lambda'(1)} \right), so \\
&G^* < 1 - e^{-G^*\Lambda'(1)}
\end{aligned} \tag{5.7}
$$

where for each value of $\Lambda'(1)$ is possible to find the corresponding G^*. The bound vs soliton distributions with different $\Lambda'(1)$ is depicted in Figure 5.3.

Naturally from the point of view of the simulation N will be a finite value (truncated).

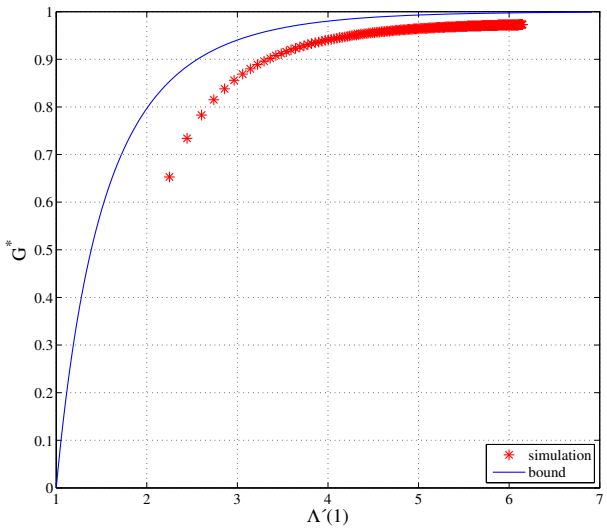

Figure 5.3: Plot of the theoretical bound vs different distribution developed by the truncated soliton distribution. In the simulation we have selected $a = 10^{-4}$, $N = 256$ and $I_{max} = 1000$.

5.3 IC Process for Rayleigh fading channel

Until this moment we have considered that a packet is correctly decoded if and only if is alone in a certain time slot (due for example to the IC process or due to the fact that only one packet is transmitted in this slot), otherwise is not possible to decode it. Now, considering fading this is not anymore true, because if one packet is alone into the slot the probability of successful decoding will depend on its SNR.

Fading introduces also a big advantage, that is the *capture effect* (see Chapter 2).

While the burst node (so the probability q) is described in the same way as in the collision channel, the analysis for the sum nodes changes in order to take into account the fading effect.

Calling

$$\gamma_n = \frac{P_0}{N + \sum_n P_i}$$

the Signal to Interference Noise Ratio referred to a certain packet chosen randomly when n interfering are considered, is possible to define the value of p at the i-th iteration as

$$p_i = \sum_{n=0}^{l-1} Pr\left\{\gamma_n < b | n\right\} Pr\{n\} \tag{5.8}$$

where l is the maximum number of edges that can be connected to a certain sum node.

Recalling equation (4.6) it is possible to show that the equation (5.8) can also be written as

$$p_i = \sum_{n=0}^{l-1} \left(1 - e^{-\frac{\gamma^*}{\Gamma}} \left[\gamma^* + 1\right]^{-n}\right) Pr\{n\}$$

When Rayleigh fading is considered the probability of having n residual interferers starting from the $l-1$ available can be written as

$$Pr\{n\} = \binom{l-1}{n} q_i^n (1 - q_i)^{l-1-n}$$

By averaging over the Poisson distribution of the edges, we obtain

$$\bar{p_i} = \sum_{l=1}^{\infty} \rho_l \sum_{n=0}^{l-1} \left(1 - e^{-\frac{\gamma^*}{\Gamma}} [\gamma^* + 1]^{-n}\right) \binom{l-1}{n} \bar{q_i}^n (1 - \bar{q_i})^{l-1-n} \tag{5.9}$$

The analysis of the IC process in presence of fading can be done iterating equations (5.1) and (5.9), where the equation (5.9) takes into account the fading effects.

5.3.1 Closed formula for p when Rayleigh fading is taken into account

We will now show how to express equation (5.9) in a compact and elegant closed formula.

After a simple variable substitution l, equation (5.9) can be written as

$$\begin{aligned} \bar{p} &= \sum_{l=0}^{\infty} \rho_l \sum_{n=0}^{l} \left(1 - e^{-\frac{\gamma^*}{\Gamma}} [\gamma^* + 1]^{-n}\right) \binom{l}{n} \bar{q}^n (1 - \bar{q})^{l-n} \qquad (5.10) \\ &= \underbrace{\sum_{l=0}^{\infty} \rho_l \sum_{n=0}^{l} \binom{l}{n} \bar{q}^n (1 - \bar{q})^{l-n}}_{A} - \underbrace{e^{-\frac{\gamma^*}{\Gamma}} \sum_{l=0}^{\infty} \rho_l \sum_{n=0}^{l} \binom{l}{n} \bar{q}^n (1 - \bar{q})^{l-n} (\gamma^* + 1)^{-n}}_{B} \end{aligned}$$

The index i has been omitted for simplicity and ρ_l is still poisson distributed after the variable substitution.

The term A, using the binomial theorem

$$(a + b)^n = \sum_{k=0}^{\infty} \binom{n}{k} a^{n-k} b^k$$

can be simplified in

$$\sum_{l=0}^{\infty} \rho_l (1 + \bar{q} - \bar{q})^l = 1 \quad \forall\, \bar{q} \in (0, 1)$$

Now lets consider the term B. We can use another time the binomial

theorem so it is possible to simplify B as

$$\bar{p} = e^{-\frac{\gamma^*}{\Gamma}} \sum_{l=0}^{\infty} \rho_l \underbrace{\sum_{n=0}^{l} \binom{l}{n} \left(\frac{\bar{q}}{\gamma^*+1}\right)^n (1-\bar{q})^{l-n}}_{\left(\frac{\bar{q}}{\gamma^*+1}+1-\bar{q}\right)^l}$$

$$\bar{p} = e^{-\frac{\gamma^*}{\Gamma}} \underbrace{\sum_{l=0}^{\infty} \rho_l \left[-\bar{q}\left(\frac{\gamma^*}{\gamma^*+1}\right)+1\right]^l}_{C}$$

where the term C represents the Poisson Probability Generating Functions. Recalling equation (5.3), after the variable substitution ρ_l will be

$$\rho_l = \frac{k^l}{l!} e^{-k}$$

where $k = \bar{G}\Lambda'(1)$ for simplicity.

Recalling moreover the Probability Generating Functions for a Poisson distribution, that is

$$\sum_{l=0}^{\infty} \rho_l z^l = e^{k(z-1)}$$

then the term C can be simply in

$$C = e^{-k\bar{q}\left(\frac{\gamma^*}{\gamma^*+1}\right)}$$

so, finally the new expression of $\bar{p}$ is

$$\bar{p} = 1 - e^{-\left(k\bar{q}\frac{\gamma^*}{\gamma^*+1}+\frac{\gamma^*}{\bar{\Gamma}}\right)} \tag{5.11}$$

The importance of having a closed formula relies in its general applicability, and its easy relation between $\bar{p}$ and k, $\bar{\Gamma}$ and γ^*.

5.3.2 IC convergence analysis for Rayleigh fading Channel

The iterative equation, used in the fading channel hypothesis are:

$$\begin{cases} q_0 = \bar{q_0} = 1 \\ \bar{p_i} = 1 - e^{-\left(k\bar{q_i}\frac{\gamma^*}{\gamma^*+1}+\frac{\gamma^*}{\bar{\Gamma}}\right)} & i = 0, ..., \infty \\ \bar{q}_{i+1} = \sum_l \lambda_l \bar{p_i}^{(l-1)} \end{cases}$$

Under fading channels we are not able to achieve vanishing error probability for $G \leq G^*$ (so that $\bar{q}, \bar{p} \to 0$), due to the presence of fading.

There is a non zero probability that a received packet cannot be correctly decoded also when it is alone in a slot.

We called now $\bar{q}$ the Extrinsic Packet Loss Probability (EPLP) and we define G^* as the maximum value of G such that

$$\bar{q} > \lambda(f_s(\bar{q})), \quad \forall\, \bar{q} \in (\delta, 1].$$

where δ represents the target EPLP and is greater than zero, whereas $f_s(\bar{q})$ represents the closed formula previously found,

$$f_s(\bar{q}) = 1 - e^{-\left(k\bar{q}\frac{\gamma^*}{\gamma^*+1}+\frac{\gamma^*}{\bar{\Gamma}}\right)}$$

In Figure 5.4 is shown the performance of CRDSA and IRSA with two different polynomial distributions taken by Table 5.1. It is possible to see that the performance of the protocol will depend on the polynomial distribution such as the collision channel but also on $\bar{\Gamma}$ and on γ^* that represent respectively the SNR of the distribution and the decoding threshold.

We can distinguish two different regions:

- The first is for low offered traffic. The fading here is dominant to the

capture effect, due to the non zero probability of correctly decoding no one packet also if only one packet is alone into a certain time slot.

Increasing $\bar{\Gamma}$, is more clear how the fading introduces a wide interval of traffic G, where is possible to find low MAC burst error probability. This probability will depend on $\bar{\Gamma}$, γ^* and on the polynomial distribution.

- When the traffic increases instead, P_L increases rapidly (how much depends by $\bar{\Gamma}$). More precisely in this region the capture effect will be dominant. In fact increasing the traffic, now more packets can be capture, each of them introduce a certain level of interference. If the interference level will be high, less will be the probability to decode the packet into a certain slot.

  It is also interesting to see that after a certain limit the performance of IRSA becomes worse than CRDSA. In fact, while CRDSA sends two replicas for each packet, IRSA with distribution $\Lambda_1(x)$ sends in mean 3.6 replicas for each packet and IRSA with distribution $\Lambda_2(x)$ sends instead on average 4.24 replicas for each packet. For high values of G, the mean number of interfering packets will be higher for IRSA, so in this case the SIC will able decoded less packets than in CRDSA.

In order to show better the two different regions discussed, I have obtained different curves of P_L for different $\bar{\Gamma}$ for the two IRSA distributions, Figure 5.5. As we can see, the floor effect (for low-medium load) is more present when $\bar{\Gamma}$ is high.

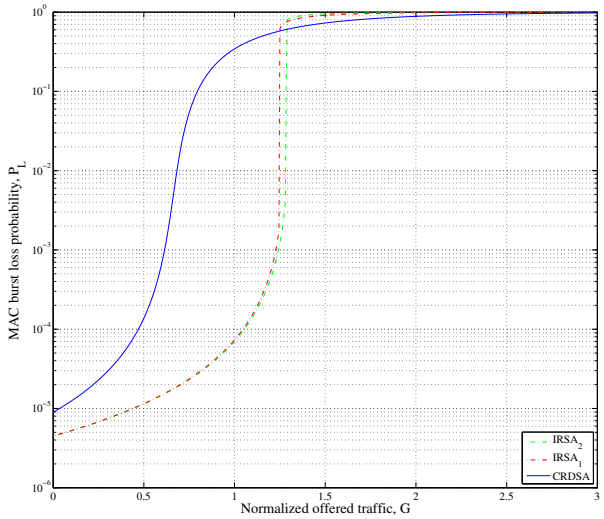

(a) Simulation for $\bar{\Gamma} = 1000$ and $\gamma^* = 3$.

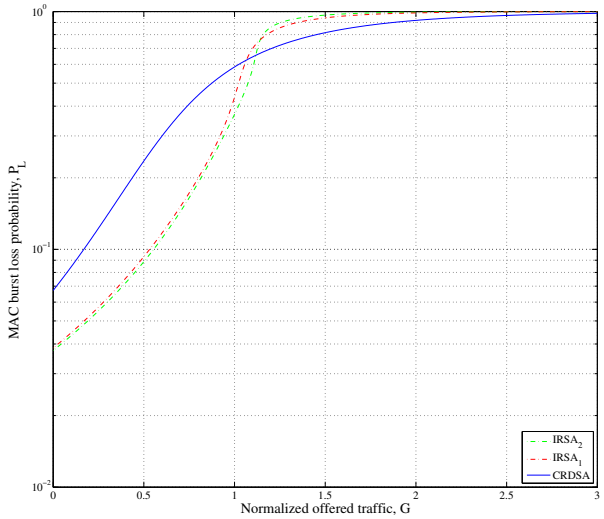

(b) Simulation for $\bar{\Gamma} = 10$ and $\gamma^* = 3$.

Figure 5.4: Asymptotic performance for CRDSA and IRSA with two irregular distribution, $\Lambda_1(x) = 0.5x^2 + 0.28x^3 + 0.22x^8$ and $\Lambda_2(x) = 0.4977x^2 + 0.2207x^3 + 0.0381x^4 + 0.0756x^5 + 0.0398x^6 + 0.0009x^7 + 0.0088x^8 + 0.0069x^9 + 0.0030x^{11} + 0.0429x^{14} + 0.0081^{15} + 0.0576x^{16}$, both obtained for $I_{max} = 1000$.

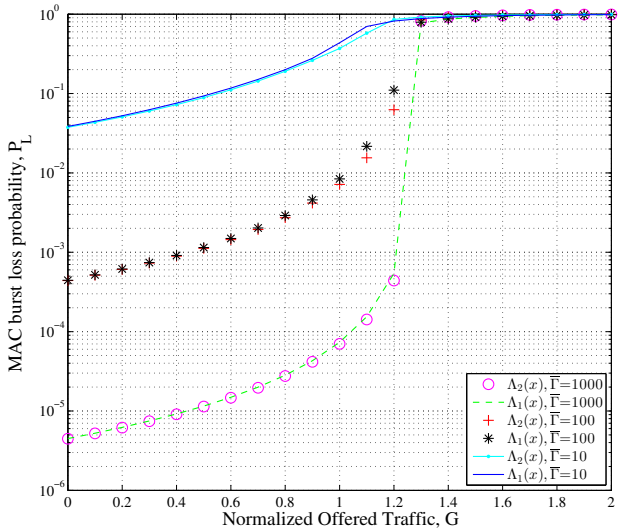

Figure 5.5: Asymptotic performance for IRSA with two irregular distribution, $\Lambda_1(x) = 0.5x^2 + 0.28x^3 + 0.22x^8$ and $\Lambda_2(x) = 0.4977x^2 + 0.2207x^3 + 0.0381x^4 + 0.0756x^5 + 0.0398x^6 + 0.0009x^7 + 0.0088x^8 + 0.0069x^9 + 0.0030x^{11} + 0.0429x^{14} + 0.0081^{15} + 0.0576x^{16}$. Both the simulation are obtained for $\gamma^* = 3$ and $I_{max} = 1000$.

5.3.3 Evaluation of the Upper Bound of P_L

Is possible to find for each distribution, the minimum value of P_L, we can call it $P_{L_{min}}$. This minimum value is obtained for $G = 0$. For traffic values very close to this value G, the probability to correctly decode no one packet depends only by the fading characteristics, then is possible to define

$$P_L(d) = (1 - e^{-\frac{\gamma^*}{\Gamma}})^d$$

where $P_L(d)$ represents the probability to decode no one packets when d replicas are sent and zero interfering users are present.

Recalling the Jensen's inequality which it says that

$$f(\mathbb{E}[X]) \leq \mathbb{E}[f(X)]$$

and applied it at our case,

$$P_L^{\mathbb{E}[d]} \leq \mathbb{E}[P_L(d)] \Rightarrow P_L^{\Lambda'(1)} \leq \sum_l \Lambda_l P_L^l$$

where $\sum_l \Lambda_l P_L^l$ can represent an upper bound to $P_{L_{min}}$.

$Example$ 1: In the CRDSA case of Figure 5.4 with $\bar{\Gamma} = 10$ and $\gamma^* = 3$ is clear as $\Lambda'(1) = 2$ so, in this case $P_L^{\Lambda'(1)} = \sum_l \Lambda_l P_L^l$, so $P_{L_{min}} = 6.72 \cdot 10^{-2}$.

$Example$ 2: In the IRSA case of Figure 5.4 with $\bar{\Gamma} = 10$ and $\gamma^* = 3$ with distribution Λ_1 is possible to evaluate with the upper bound the $P_{L_{min}}$ value, then $P_L = \sum_l \Lambda_l P_L^l$, so $P_{L_{min}} = 3.85 \cdot 10^{-2}$.

More the $\bar{\Gamma}$ will be high and more the $P_L(d)$ is low.

5.3.4 Simulation for different distribution vs theoretical bound for fading channel

Starting from the observation done for the collision channel, is possible to enlarge here the definition on the upper bound previously discussed. An open tunnel must exist between $f_s(q)$ and $f_b(p)$, but this time q and p will not go to zero; moreover the G^* will depend on the probability target δ. For the consideration just done, the condition which guarantees that the packets are correctly decoded (until a certain probability of error that is depends by δ) is given now by $A_s + A_b < 1 + \delta f_s(\delta)$ where $\delta f_s(\delta)$ represents the area which will be subtracted from the integral of the functions. While A_b is still equation (5.6), A_s is described now by

$$\begin{aligned} A_s &= \int_0^1 1 - e^{-\left(k\bar{q}\frac{\gamma^*}{\gamma^*+1}+\frac{\gamma^*}{\Gamma}\right)} \; dq \\ &= \int_0^1 1 \; dq - e^{-\frac{\gamma^*}{\Gamma}} \int_0^1 e^{-\frac{k\gamma^* q}{1+\gamma^*}} \; dq \\ &= 1 + e^{-\frac{\gamma^*}{\Gamma}} \left[\frac{e^{-\frac{k\gamma^* q}{1+\gamma^*}}}{\frac{k\gamma^*}{1+\gamma^*}} \right]_0^1 \\ &= 1 + e^{-\frac{\gamma^*}{\Gamma}} \left[\frac{1+\gamma^*}{k\gamma^*} \left(e^{-\frac{k\gamma^*}{1+\gamma^*}} - 1 \right) \right] \\ &= 1 - \left(\frac{1+\gamma^*}{\gamma^* k} \right) \left(1 - e^{-\frac{k\gamma^*}{1+\gamma^*}} \right) e^{-\frac{\gamma^*}{\Gamma}} \end{aligned}$$

so our bound can be described as,

$$\begin{aligned} &1 - \left(\frac{1+\gamma^*}{\gamma^* k} \right) \left(1 - e^{-\frac{k\gamma^*}{1+\gamma^*}} \right) e^{-\frac{\gamma^*}{\Gamma}} + \frac{1}{\Lambda'(1)} < 1 + \delta f s(\delta) \\ &- e^{\frac{\gamma^*}{\Gamma}} \left(\delta f_s(\delta) - \frac{1}{\Lambda'(1)} \right) < \frac{\gamma^*+1}{k\gamma^*} \left(1 - e^{-\frac{k\gamma^*}{\gamma^*+1}} \right) \end{aligned} \tag{5.12}$$

Equation (5.12), cannot be expressed in closed form, unfortunately. Using the Matlab tools we have evaluated numerically the values of G (fixed $\Lambda'(1)$) that satisfy equation (5.12), this is represented in Figure 5.6.

The different polynomial distributions are realized from the truncated soliton distributions with fixed parameters a, N and target δ.

In Figure 5.6 is shown this case, where is possible to see that the simulation points are under the bound.

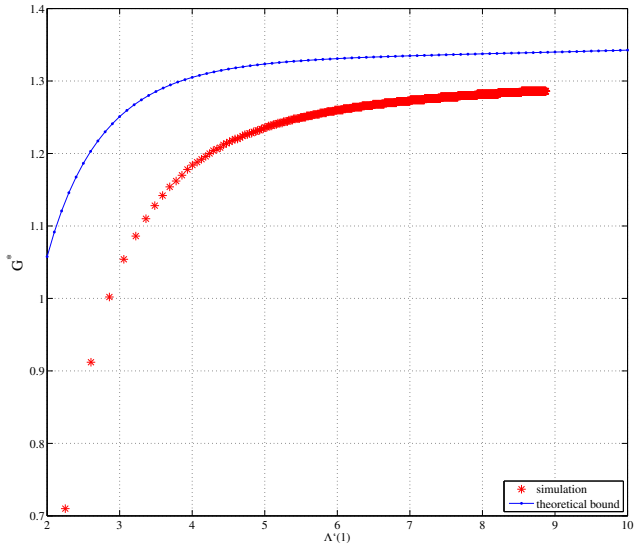

Figure 5.6: Plot of the theoretical bound when the fading is taken into account vs different distribution developed by the truncated soliton distribution. For the simulations we have chosen $a = 10^{-4}$, $N = 256$, $I_{max} = 1000$, $\delta = 10^{-2}$, $\bar{\Gamma} = 30$ dB and $\gamma^* = 4.7$ dB.

5.3.5 Example of good degree distribution

It has been possible to find some good degree distributions taking into account the characteristics of the fading channel using the Genetic Algorithms [27].

The main idea for explaining how this kind of algorithms work, can be described as follows. All start from a random population composed by a certain number of polynomial distribution where each distribution has the same maximum degree. Each distribution joins with a random distribution partner and their result consist into a generation of two new polynomial distributions. Each one has new Λ_l derived by the mean of the Λ_l of their parents with a certain probability called cross over probability P_c, or it assumes the same value Λ_l at one of the parents, with probability $1 - P_c$. When the new Λ_l is generated by the mean of the corresponding Λ_l

parents, is also possible to introduce a certain degree of aleatority, which one can be controlled by the amplification factor. Each of the new polynomial distribution has a certain threshold G^* that is compared with the threshold of the departed distribution. If the new one is higher than the started threshold, the distribution just created is used for the successive generations, otherwise the new one will be discarded.

We show in the next some different polynomial distributions obtained for the same maximum degree of the distributions listed in Table 5.1, with different fading conditions. The results are shown in Table 5.2, 5.3 and Table 5.4.

The first observation can be done is that, increase the mean number of replicas for each transmitted packet, it consist to obtain an increase G^* value. Increase the mean rate of the distribution corresponds at increase the maximum degree of the distribution. It is also possible to see that, the increase of the performance depend on the fading conditions. In Table 5.2 it is remarkable the G^* gain achieved increasing the maximum polynomial degree (and so the mean repetition of transmitted replicas). In particular, the results are referred at $\bar{\Gamma} = 10$ and $\gamma^* = 3$.

Distribution, $\Lambda(x)$	G^*	$\Lambda'(1)$
$0.0103x^2 + 0.9897x^3$	0.342	2.99
$0.5005x^3 + 0.4995x^4$	0.749	3.49
$0.2774x^2 + 0.0159x^3 + 0.1431x^4 + 0.5610x^5 + 0.0026x^6$	0.908	3.99
$0.3819x^2 + 0.0027x^3 + 0.0289x^4 +$ $0.2860x^5 + 0.0909x^6 + 0.0497x^7 + 0.1598x^8$	0.938	4.48
$0.2832^2 + 0.3859x^4 + 0.1708x^5 + 0.0304x^7 +$ $0.0096x^{11} + 0.0079x^{12} + 0.0188x^{15} + 0.0933x^{16}$	0.968	5.15

Table 5.2: Thresholds computed for different distributions, fixed $\bar{\Gamma} = 10$, $\gamma^* = 3$, $I_{max} = 1000$ and $\delta = 10^{-1}$.

If we observe Table 5.3 and Table 5.4 instead, we can see that these table have almost the same results. The reasons of this, could be that, $\bar{\Gamma} = 100$ represents a good value of SNR yet.

Moreover we can also observe by these table that, increasing the maximum polynomial degree, make only a sightly increase of G^*.

Distribution, $\Lambda(x)$	G^*	$\Lambda'(1)$
$0.5229x^2 + 0.4771x^4$	1.12	2.95
$0.5779x^2 + 0.4221x^5$	1.175	3.26
$0.5701x^2 + 0.0573x^3 + 0.0035x^5 + 0.3692x^6$	1.193	3.54
$0.4499x^2 + 0.3264x^3 + 0.0048x^6 + 0.0135x^7 + 0.2055x^8$	1.215	3.64
$0.4733x^2 + 0.1211x^3 + 0.2279x^4 + 0.0549x^5 + 0.0013x^6 +$ $0.0019x^7 + 0.0054x^8 + 0.0033x^{10} + 0.0369x^{14} + 0.0741x^{16}$	1.254	4.28

Table 5.3: Thresholds computed for different distributions, fixed $\bar{\Gamma} = 100$, $\gamma^* = 3$, $I_{max} = 1000$ and $\delta = 10^{-1}$.

Distribution, $\Lambda(x)$	G^*	$\Lambda'(1)$
$0.5353x^2 + 0.4647x^4$	1.154	2.92
$0.6153x^2 + 0.3847x^5$	1.20	3.15
$0.6013x^2 + 0.0494x^3 + 0.0089x^4 + 0.0074x^5 + 0.3330x^6$	1.225	3.42
$0.5042x^2 + 0.2713x^3 + 0.0022x^4 + 0.0081x^6 + 0.2142x^8$	1.249	3.59
$0.4905x^2 + 0.2187x^3 + 0.0912x^4 + 0.0163x^5 +$ $0.0342x^6 + 0.0229x^7 + 0.0278x^8 + 0.0144x^9 +$ $0.0026x^{11} + 0.0034x^{13} + 0.0415x^{15} + 0.0367x^{16}$	1.283	4.08

Table 5.4: Thresholds computed for different distributions, fixed $\bar{\Gamma} = 1000$, $\gamma^* = 3$, $I_{max} = 1000$ and $\delta = 10^{-1}$.

Chapter 6

Numerical results

Our simulator has been develop with MATLAB. Users transmission are organized into MAC frames each one composed by N_{slots}. The medium is shared by a finite population of m users. Each user is active with probability p, equal for all users; i.e. it decides whether to send a packet in the current MAC frame with probability p. The offered traffic load G, the number of slots in a frame N_{slot}, the probability p and the user number m are related by the following expression, $p = \frac{G \cdot N_{slot}}{m}$.

The throughput of each protocol S, has been analyzed, where for throughput I mean the number of packets correctly received over the number of transmitted packets. Moreover it has been simulated and computed as the mean over a certain number of simulations N_{sim}, for each value of traffic load G.

In our simulations, , fading aspects are also taken into account.

We recall that we have assumed a Rayleigh fading which results in a exponential distribution of the received power. We have assumed that the received power associated to each packet is a random variable, i.i.d., that follow equation (2.2).

For each simulation we will propose later, there will be a description of the simulation parameters that have been used.

The definition of the simulation parameters is summarized in Table 6.1:

Simulation parameters	Significate
m	Total number of users
N_{slot}	Number of slot into the MAC frame
N_{sim}	Number of simulation for each channel load value
I_{max}	Number of maximum iterations of SIC
$\bar{\Gamma}$	mean SNR of the Rayleigh distribution
γ^*	decoding threshold

Table 6.1: Simulations parameters in our simulator.

6.1 SA with Rayleigh fading channel

Here the performance of SA with Rayleigh fading channel has been considered. The two Figures, precisely Figure 6.1 and 6.2 shown a dual behavior, in fact in the first picture we have fixed the decoding threshold γ^* and the results are showed for different values of SNR $\bar{\Gamma}$, while in the second figure we have done the opposite.

As we can see in Figure 6.1, the curves are different from the well-know curve of SA under the collision channel hypothesis. In particular we can observe that both throughput peak and corresponding channel load differ from the values of 0.36 and of $G = 1$. These values, naturally will depend on the SNR value of the distribution and on the threshold.

For very low values of traffic, the throughput is linear with G so it is possible to obtain low packet loss rates and low transmissions delay. With respect to SA, here we have a slightly better performance if the level of SNR exceeds the threshold level. The throughput peak instead, can be significantly higher in the fading channel hypothesis and this normally appear for G quite high. Different peak values have been obtained, as we can see from the Figure 6.1.

Briefly, we can say that when the channel conditions are good (the mean level of power distribution) or else when the SNR is much higher than threshold level, we can achieve higher value of throughput.

Otherwise, when instead the SNR is close to the threshold, we could obtained worse performance than the SA, because is more probable that the SINR corresponding at certain packet, is less than the threshold.

For high value of offered traffic the level of interference increases caus-

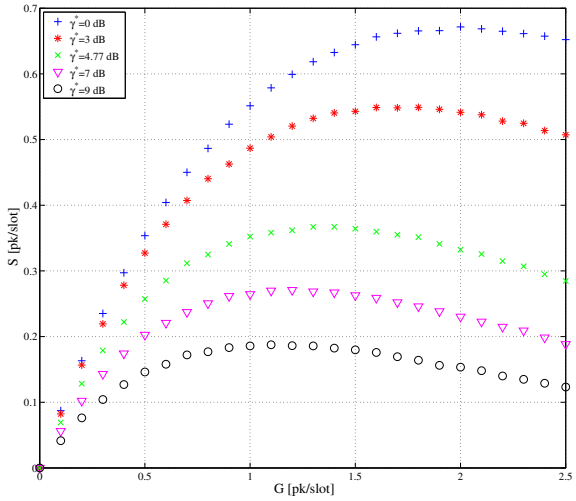

Figure 6.1: Throughput of SA, taking into account the effect of Rayleigh fading. We fixed the $\bar{\Gamma} = 10$ dB and $\gamma^* = 0, 3, 4.77, 7, 9$ in dB. Each value of G has been simulated for $N_{sim} = 2000$.

ing more collisions that reduce the average SINR and therefore the probabilty of exceeding the threshold is reduced.

These behaviors are depicted in Figure 6.1 and 6.2.

We have neglected the phase associated at the received power for packet (recalling equation (2.3)), then the total interfering power has been obtained as the sum of the single interfering power.

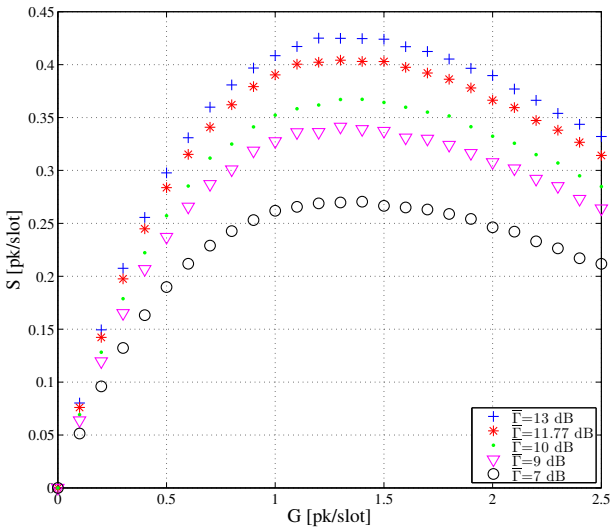

Figure 6.2: Throughput of SA under Rayleigh fading. We fixed $\gamma^* = 4.77$ dB and $\bar{\Gamma} = 13, 11.77, 10, 9, 7$ in dB. Each value of G has been simulated for $N_{sim} = 2000$.

6.2 CRDSA

CRDSA protocol has been introduced in Chapter 1 and now we want to show its performance. The simulations have been done for first referred at the collision channel case, after that the fading case is considered. The simulation scenario has been introduced at the start of this Chapter.

6.2.1 CRDSA for Collision Channel

As a first step we have evaluated CRDSA under the collision channel hypothesis. In Figure 6.3 we have shown the results. In comparison with SA, it is easy to show how this protocol has a better performance (for low-medium load) also in absence of fading.

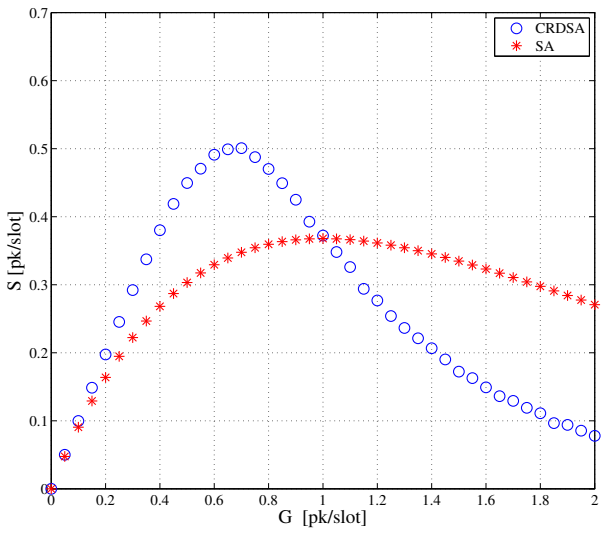

Figure 6.3: CRDSA protocol under the collision channel hypothesis. We have chosen $N_{slot} = 50$, $N_{sim} = 1800$, $m = 1000$ users and $I_{max} = 20$.

We can observe that the throughput performance are definitely better than the SA protocol until $G = 1$. Specifically, the value of the peak throughput exceeds 0.5 [pk/slots]. Compared to the peak throughput of SA, i.e. 0.36, this is a $\simeq 45\%$ improvement.

From Figure 6.3 it is clear how the protocol has a good behavior for low offered traffic, this is due to the transmission of two replicas for each

packet and thanks to the presence of SIC at the receiver. In this region, we are able to obtain better packet transmission delays and loss probabilities with respect to SA.

After the SA peak, CRDSA results in a deterioration of its performance, and the SA has here better throughput values. The reason of this, can be reconducted at the number of transmitted packets. In fact, the CRDSA aries on the transmission of two replicas for each packet, so when the traffic load increases, too many packets are send into the channel due to CRDSA. Then, if more than one packets are into a certain slot, the SIC can not correctly decoded the packet and can not erase its power interference.

From Figure 6.4 is possible to see a differences in throughput terms when N_{slot} changes, specially for the range of traffic load near the peak value. When we consider low value of G the number of slots do not influence the performance. This happen because the transmissions are very few. When instead we consider a traffic load around the peak value, have a high number of slots consist in an improvement of the throughput. Increasing N_{slot}, consist also in an increase the p value, then when the number of slots is sufficiently big (i.e. $N_{slot} \geq 500$) the throughput does not change anymore.

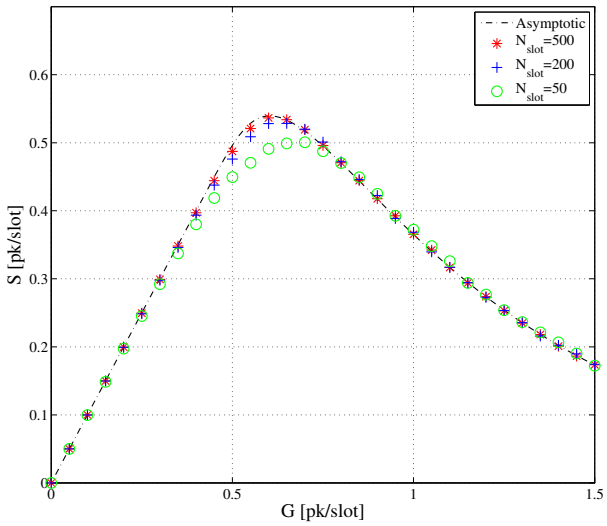

Figure 6.4: CRDSA protocol under the collision channel hypothesis with $N_{slot} = 50, 200, 500$. We have chosen $N_{sim} = 1800$, $m = 1000$ users and $I_{max} = 20$.

6.2.2 CRDSA under Rayleigh fading Channel

More interesting is understand what happens to the performance when the Rayleigh fading is taken into account. In Figure 6.5 and Figure 6.6 we have represented this case.

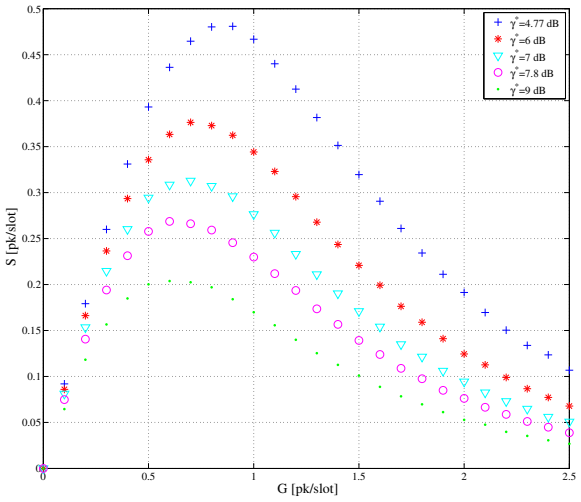

Figure 6.5: Throughput of CRDSA. We have fixed $N_{slot} = 100$, $N_{sim} = 1500$, $\bar{\Gamma} = 10$ dB and $\gamma^* = 4.77, 6, 7, 7.8, 9$ dB.

For low value of G the throughput is linear with the offered traffic, this would say intuitively that the packet loss rate (and also the transmission delays) is low.

The value of the maximum throughput achievable will depend on the parameter of the channel, precisely by the level of fading (SNR value) and by threshold γ^* selected.

The higher the SNR the higher will be the maximum throughput, for a fixed γ^*.

As we could expect, when the threshold value increases (fixed $\bar{\Gamma}$), the maximum throughput decreases. This happened because increasing γ^* would mean that we will have less packets able to have their SINR greater than the threshold.

We can see the same behavior of Figure 6.5 in Figure 6.6 where this one is obtained for varying the SNR instead of γ^*.

In Figure 6.7 we have shown the throughput for different sizes of MAC

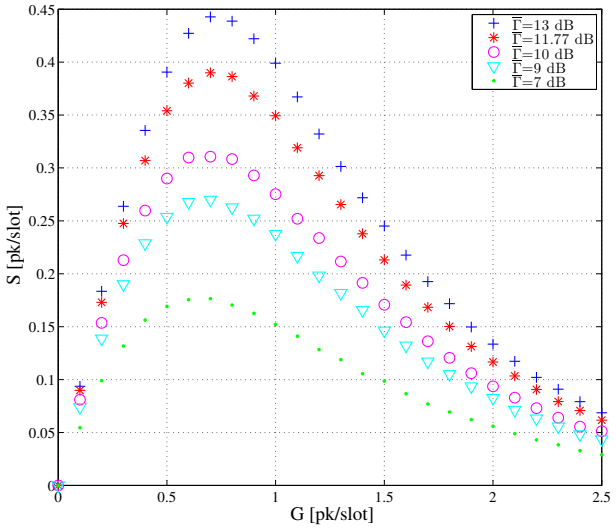

Figure 6.6: Throughput of CRDSA. We have fixed $N_{slot} = 100$, $N_{sim} = 1500$, $\gamma^* = 7$ dB and $\bar{\Gamma} = 13, 11.77, 10, 9, 7$ dB.

frames, and we can observe that only minor changes in the curves are given.

Another interesting comparison is the one between CRDSA and SA under Raylegih fading.

In Figure 6.8 is depicted this case, where, we have been showing that sending the same packet twice slightly improves the probability of transmission success (i.e no collision) for small MAC loads. As we can see the CRDSA protocol is better in terms of throughput if we are under a certain value of G', that in the figure is located close to $G = 1.4$ [packets/slot], otherwise its performance are worse than the SA.

When the traffic load exceeds G', it is evident that the interference has became too high for allowing the correct decoding of the packets. Moreover the performance of SA taking into account the Fading result in an improvement of its performance with respect to the SA case.

It is also possible to analyze through the IC techniques which is the SINR probability distribution before and after the possible cancellation of interference. Loosely speaking, we will observe the distribution of SINR when the MAC frame is received and after the procedure of SIC where the curves associated at these two different probability distribution are called

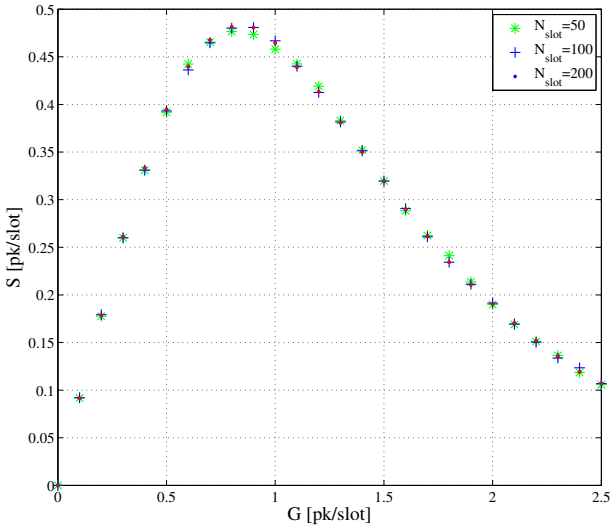

Figure 6.7: Throughput of CRDSA for different slot length. In our cases $N_{slot} = 50, 100, 200$. We have assumed $N_{sim} = 1500$, $\bar{\Gamma} = 10$ dB and $\gamma^* = 4.77$ dB.

respectively a and b.

What can be observed in Figure 6.9 and Figure 6.10 is the fact that after the SIC procedures (curve b) we have an higher probability to find high SINR than the curve a. This happened because, the SIC can erases some (even all) packets collided mainly when we consider medium traffic conditions. If we focus in a certain slot, the level of interference decreases and is more probable to find packets with their SINR greater than their SINR associated at curve a.

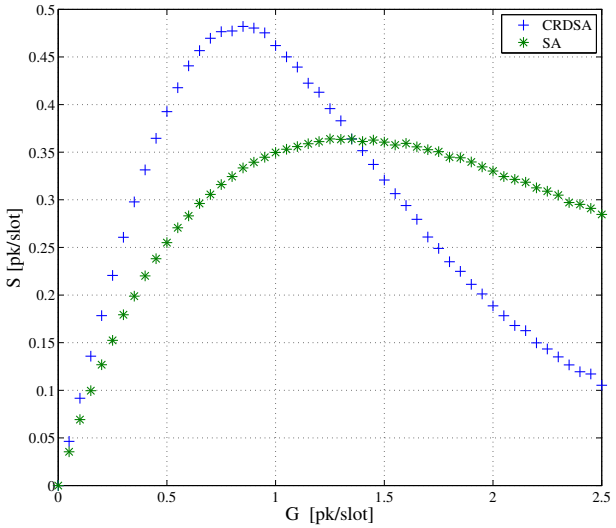

Figure 6.8: Throughput of CRDSA vs Slotted ALOHA with capture phenomenon. We have fixed $N_{slot} = 100$, $\overline{\Gamma} = 10$ dB and $\gamma^* = 4.77$ dB.

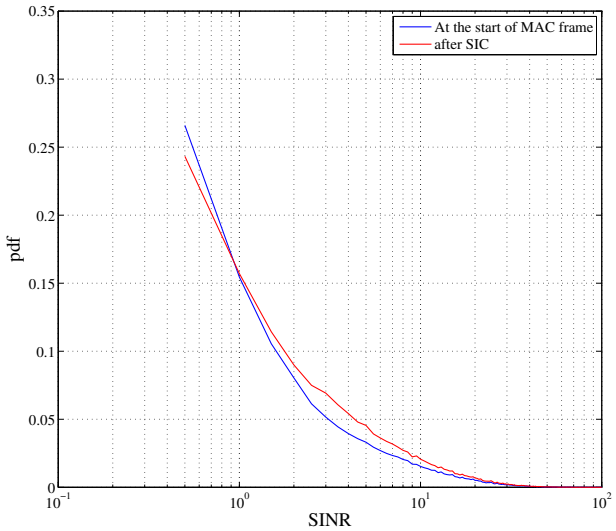

Figure 6.9: Probability density function of the SINR at the starting of the MAC frame and after the SIC iterations. The curves are obtained for $G = 0.5$ [pk/slot] and $\bar{\Gamma} = 10$ dB and $\gamma^* = 4.77$ dB.

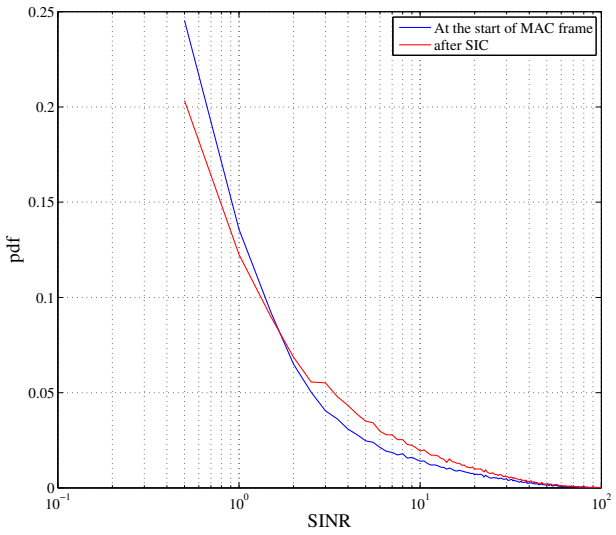

Figure 6.10: Probability density function of the SINR at the starting of the MAC frame and after the SIC iterations. The curves are obtained for $G = 0.5$ [pk/slot] and $\bar{\Gamma} =$ 13 dB and $\gamma^* = 4.77$ dB.

6.3 IRSA

The performance of IRSA are now considered. Such as for the CRDSA, here we evaluated the throughput performance vs the offered traffic G for a finite number of users m and for a finite number of slots N_{slot}, in different cases.

6.3.1 IRSA for Collision Channel

The first simulation in Figure 6.11 has the aim to show the throughput of IRSA, compared to the one of CRDSA and SA, assuming a fixed number of slot $N_{slot} = 50$ and for different values of iteration I_{max}. The results of the simulation shows that with $I_{max} = 100$, IRSA has a throughput close to $S \simeq 0.6$ while CRDSA does not exceed the value of $S \simeq 0.5$. Then, IRSA consists in a gain of $\simeq 20\%$ respect CRDSA and in a gain of $\simeq 60\%$ than SA. IRSA achieves better throughput performance, due to the mean repetition rate for each transmitted packet, that is greater than SA and CRDSA. In particular the distribution at which we referred is $\Lambda_1(x)$ which has mean value of the repetition fixed to 3.6.

Considering the results achieved for $I_{max} = 10$ that represents the case of low complexity implementations [4], IRSA does not seem have particular degradation with respect to the previous case. We can see by the figure that the throughput vs the traffic offered is going linear up to $S \simeq 0.5$, so all the traffic up to this G turns into throughput, obtaining vanishing error probability. It is to markable the fact that here we have chosen a small number of slot for MAC frame, this choice impacts the throughput's peak, as you can see in Figure 6.12 where the performance of IRSA for different number of N_{slot} are shown.

Continuing to observe Figure 6.11, for value of G close to one we can observe two phenomenons; the first is the fact that for G over G^* the simulated point falls outside the Theoretical curve of IRSA. This happened because with a finite MAC frame, is possible to correctly decode the packet, also after the G^* value. The asymptotic case assumes instead, that after the G^* value, the probability to correctly decode the packet is zero. Then, in this region and for a finite number N_{slot}, we can find a throughput better than the theoretical curve.

The second aspect regards the fact that there are no advantage to use IRSA instead of SA and CRDSA. This happened because the number of the replicas (into the physical load) are too much compared with the burst of SA scheme for example, so this results in a high packet loss rate. Where the IRSA becomes worst than the others protocol is depends (as previously discussed) by the polynomial distribution used for the replicas.

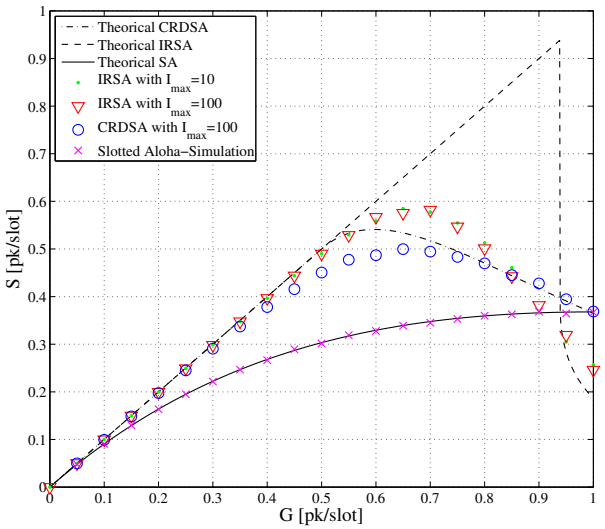

Figure 6.11: Throughput of IRSA with polynomial distribution $\Lambda_1(x) = 0.5x^2 + 0.28x^3 + 0.22x^8$ compared with the CRDSA and SA performance, for different value of I_{max}. We have chosen $m = 1000$, $N_{slot} = 50$, $I_{max} = 100, 10$ and $N_{sim} = 1500$.

In Figure 6.12 we depicted the performance of the IRSA protocol for different numbers of N_{slot}, where we have fixed the number of iteration to $I_{max} = 20$. We can see that increasing the number of slots, the performance increases significantly than the previous case with $N_{slot} = 50$. It is clearly that when the number of the slots increases significantly we are going to the asymptotic performance, so we are able to turns all the offered traffic into throughput until $G = 0.938$ that represents the G^* for the considered distribution.

In this figure is also depicted the throughput of CRDSA with $N_{slot} = 500$. As we can see, if we increase the number of slots, also the CRDSA performance increases. Moreover, this case is almost coincident with its asymp-

totic limit. Nevertheless, CRDSA with $N_{slot} = 500$ has worse throughput performance than IRSA, also for IRSA with $N_{slot} = 50$.

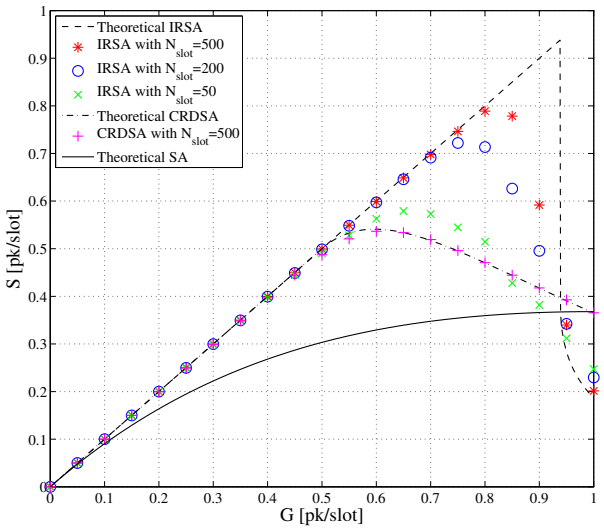

Figure 6.12: Throughput of IRSA with polynomial distribution $\Lambda_1(x) = 0.5x^2 + 0.28x^3 + 0.22x^8$ vs the offered traffic, for different value of N_{slot}. We have chosen $m = 1000$, $I_{max} = 20$, $N_{sim} = 2000$ and $N_{slot} = 500, 200, 50$.

6.3.2 IRSA for Rayleigh fading channel

Now also for IRSA we want to take into account the effects of the fading.

As a first result we show the throughput for different values of $\bar{\Gamma}$. If $\bar{\Gamma}$ is high, we are able to exceed the value of 1 [pk/slot], that represents the maximum throughput value achievable under the collision channel hypothesis. The results are shown in Figure 6.13.

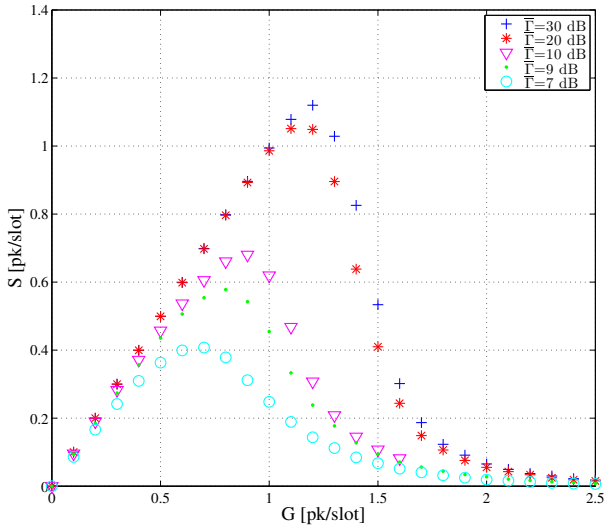

Figure 6.13: Throughput of IRSA with polynomial distribution $\Lambda_1(x) = 0.5x^2 + 0.28x^3 + 0.22x^8$ vs the offered traffic, for different value of $\bar{\Gamma}$. We have chosen $m = 1000$, $N_{slot} = 100$, $I_{max} = 20$, $N_{sim} = 1500$. Moreover we have fixed $\gamma^* = 4.77$ dB and $\bar{\Gamma} = 30, 20, 10, 9, 7$ dB.

How is possible to see the performance of the protocol will be depend on the mean level of the power's distribution and by the level of fixed threshold for the system. For $\bar{\Gamma}$ very close to γ^*, this condition represents the situation in which the capture of the received packet will be difficult, also for low-medium offered traffic. In this case the capture effect does not provide any kind of help and the throughput can be also worst than the collision channel case.

By the Figure 6.14 is possible to see that fixed these channel condition the chose number of the SIC iteration, does not impact on the performance of the protocol (for I_{max} greater equal to 10); this is important because at

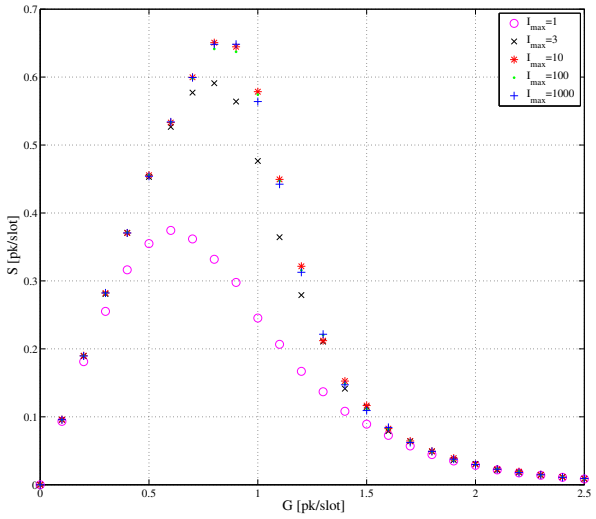

Figure 6.14: Throughput of IRSA with polynomial distribution $\Lambda_1(x) = 0.5x^2 + 0.28x^3 + 0.22x^8$ vs the offered traffic, for different value of I_{max}. In particular we have fixed $N_{slot} = 100$, $N_{sim} = 1500$, $m = 1000$, $\bar{\Gamma} = 10$ dB, $\gamma^* = 4.77$ dB and $I_{max} = 1000, 100, 10$.

the increasing of I_{max} increase the delay associated at the software elaboration done at the receiver. The delay associated at the software elaboration done at the receiver is not analyze in this thesis, we can say only an approximate considerations.

In Figure 6.15, we have shown what happen at the performance for different number of slot such as in the collision channel. The increase number of slots consist in an increasing of the throughput. The peak is not so high because the fading condition are not too much well, otherwise we can imagine the same behavior of the throughput but shifted to the up when $\bar{\Gamma}$ is higher than the chosen value.

In Figure 6.16, 6.17 and 6.18 is shown the throughput performance for the distribution found in Table 5.2, Table 5.3 and Table 5.4, respectively. The distributions index i used in figures, represents the distribution in the i-th row of the Table at which we referred.

Figure 6.16 shows that, increase the mean number of transmitted replicas $\Lambda'(1)$, consist to achieve better throughput performance. Precisely, for the different distributions with $\Lambda'(1)$ up to 4.48, we have not any kind of

gain in throughput terms, respect the collision channel case. In fact, for these distributions, the maximum peak values not exceed value 0.6. Considering instead, the distribution with highest $\Lambda'(1)$ of Table 5.2, the peak is almost 0.7, resulting in a gain respect the collision channel case. However, the performance here, are subjected to a degradation than the asymptotic results. This because a limited number of slots is considered ($N_{slot} = 50$).

The behavior of the distributions change when we consider value of traffic quite high. In fact here, the distributions with high $\Lambda'(1)$ suffer of high level of interference, then more collided packet will be lost.

In Figure 6.17 and Figure 6.18 a high number of slots is considered ($N_{slot} = 500$). The results show that the peaks of the different distributions are very closed, confirming the asymptotic results achieved in section 5.3.5. It is remarkable the fact that we are able to achieved a throughput greater than one packet for slot, resulting in a gain respect the collision channel case. After the peak, the distributions with high mean number of replicas suffer an a high performance degradation than the distributions with less mean rate of repetition.

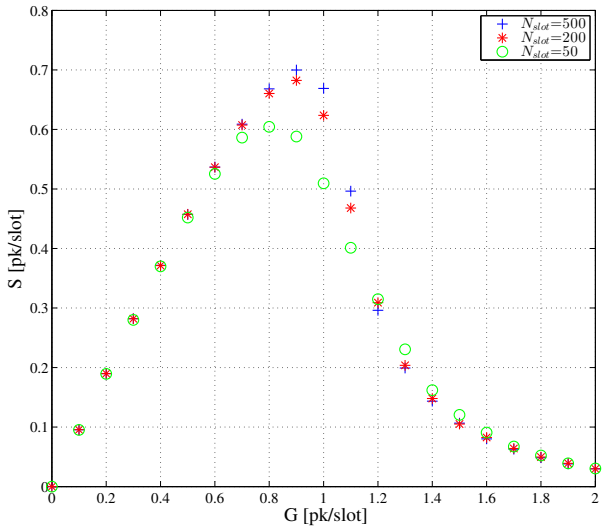

Figure 6.15: Throughput of IRSA with polynomial distribution $\Lambda_1(x) = 0.5x^2 + 0.28x^3 + 0.22x^8$ vs the offered traffic, for different value of N_{slot}. In particular we have fixed $I_{max} = 20$, $N_{sim} = 1500$, $m = 1000$, $\bar{\Gamma} = 10$ dB, $\gamma^* = 4.77$ dB and $N_{slot} = 500, 200, 50$.

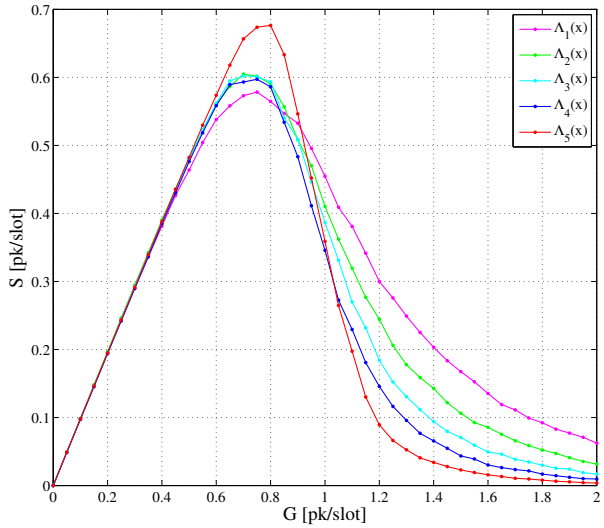

Figure 6.16: Throughput of IRSA referred at the distribution in Table 5.2. We have chosen $m = 1000$, $N_{sim} = 1500$ and $N_{slot} = 50$.

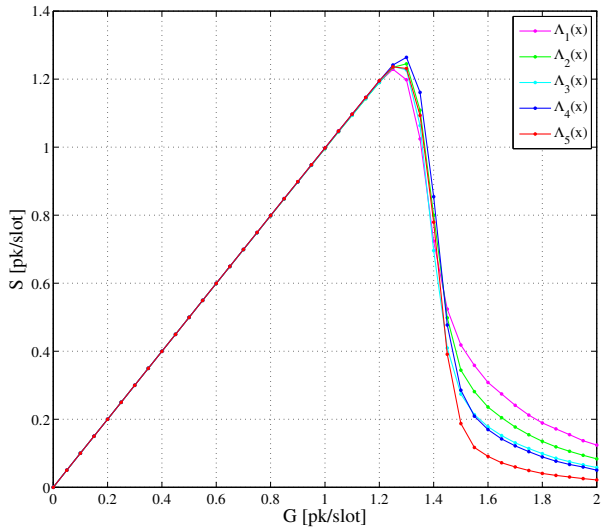

Figure 6.17: Throughput of IRSA with polynomial distribution referred at the distribution of Table 5.3. We have chosen $m = 1000$, $N_{sim} = 1500$ and $N_{slot} = 500$.

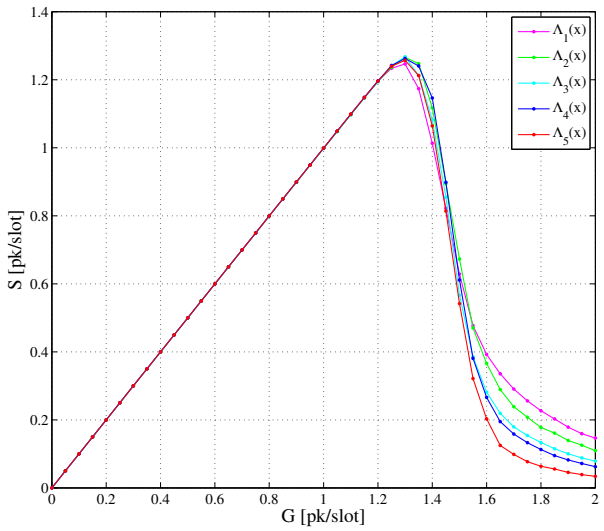

Figure 6.18: Throughput of IRSA with polynomial distribution referred at the distribution of Table 5.4. We have chosen $m = 1000$, $N_{sim} = 1500$ and $N_{slot} = 500$.

Conclusions

The main goal of this thesis has been to analyze the asymptotic performance of the IC process under the fading channel hypothesis, for IRSA protocol. Precisely we have considered the fading as a Rayleigh distributed. Actually, this kind of analysis is absent in literature.

From the asymptotic results obtained, different good polynomial distributions under different fading conditions have been investigated and found. Moreover, starting from these, the performance of IRSA for finite MAC frames have been evaluated, which are very interest in a practical case.

From our distributions studied, it is possible to say that, increase the mean number of replicas for each transmitted packet, its consist always to increase the performance (for our mean value).

The results show that the good distributions found, have a good behavior also for a finite MAC frames.

The results have also shown that in particular fading conditions, a throughput greater than one packet for slot has been achieved, resulting in an improvement respect the collision channel case.

It has been possible to show that, if the fading is not to much far from the threshold level decoding, better performance can be achieved increasing the mean number of replicas for each transmitted packet. Otherwise, when the fading level is quite high than the threshold, increase the mean number of replicas consist only in a sightly increase of performance. Nevertheless, when the traffic offered is high the distribution with high repetition rate suffer of high level of interference. Then, the distribution must be chosen take into account also for which values of traffic the system should work.

From these studies done, the next step could be evaluate the perfor-

mance of IRSA protocol in a real environment, showing the difference among the practical case and the simulation results.

Another interesting aspect could be the study of the performance under another fading model, i.e. Rice distributed. Sure, one of the most interesting things found with this work is the possibility to describe the IC process with quite easy equations. This is due to the closed formula of the probability to correctly decode no one packet into a certain slot, found for the Rayleigh distribution. Another model, could not have, this kind of characteristics.

Acronyms

RA	Random Access
DSA	Diversity Slotted ALOHA
DAMA	Demand Assignment Multiple Access protocol
CRDSA	Contention Resolution Diversity Slotted ALOHA
IRSA	Irregular Repetition Slotted ALOHA
CSA	Coded Slotted ALOHA
DVB-RCS	Digital Video Broadcasting Return Channel via Satellite
TIA	Telecommunication Industry Association
IPoS	IP over Satellite
AWGN	Additive White Gaussian Noise
AIS	Automatic Identification System
EPLP	Extrinsic Packet Loss Probability
IC	Interference Cancellation
PER	Packet Error Rate
MAC	Medium Access Control
SIC	Successive Interference Cancellation
BER	Bit Error Rate

SNR	Signal to Noise Ratio
SINR	Signal to Interference Noise Ratio
GMSK	Gaussian Minimum Shift King
CRC	Cyclic Redundancy Check

Bibliography

[1] N. Abramson, *"The Throughput of Packet Broadcasting Channels"*,IEEE transactions on communications, vol. Com-25, No.1, January 1977.

[2] Gagan L. Choudhury, Stephen S. Rappaport, *"Diversity Slotted Aloha - A Random Access Scheme for Satellite Communications"* , IEEE transactions on communications, vol. com-31, No.3, March 1983.

[3] T. Le-Ngoc and J. I. Mohammed, *"Combined free/demand assignment multiple access (CFDAMA) protocols for packet satellite communications; Universal personal communications,"* in Proc. 2nd International Conf. Pers. Commun., Oct. 1993, vol. 2, pp. 824-828.

[4] E. Casini, R. de Gaudenzi and O. del Rio Herrero *"Contention Resolution Diversity Slotted Aloha (CRDSA): An Enhanced Random Access Scheme for Satellite Access Packet Networks"*, IEEE transactions on wireless communications, vol. 6, No.4, April 2007.

[5] T. M. Cover, Some Advances in Broadcast Channels, chapter in the book, *"Advances in Communication Theory"*, vol. 4, edited by A. J. Viterbi. Academic Press, 1975.

[6] S. Verdú, *"Multiuser Detection"*. Cambridge University Press, 1998, chapter 7.

[7] A. J. Viterbi, *"Very low rate convolutional codes for maximum theoretical performance of spread-spectrum multiple-access channels,"* IEEE J. Sel. Areas Commun., vol. 8, no. 4, pp. 641-649, May 1990.

[8] P. Patel and J. Holtzman, *"Analysis of a simple successive interference cancellation scheme in a DS/CDMA system,"* IEEE J. Sel. Areas Commun., vol. 12, no. 5, pp. 796-807, June 1994.

[9] Digital Video Broadcasting (DVB); Interaction Channel for Satellite Distribution Systems, European Telecommunication Standardisation Institute (ETSI) EN 301 790 V1.4.1 (2005-09).

[10] IP Over Satellite, Telecommunication Industry Association TIA-1008, Oct. 2003.

[11] M. Fine and F. A. Tobagi, *"Demand Assignment Multiple Access Schemes in Broadcast Bus Local Area Networks"*, IEEE transactions on computers, vol. C-33, No.12, December 1984.

[12] H. Peyravi, *"Medium Access Control Protocols Performance in Satellite Communications"*, IEEE communications magazine, March 1999.

[13] F. Clazzer, *"Study and performance evaluation of MF-TDMA Based Random Access schemes using Successive Interference Cancellation "*, Master Thesis, January, 2012.

[14] John G. Proakis, M. Salehi *"Digital Communications"*, McGraw-Hill Higher Education, fifth edition, 2008.

[15] S. Benedetto, E. Biglieri *"Principles of Digital Transmission With Wireless Applications"*, Series Editor: Jack Keil Wolf, University of California at San Diego.

[16] *"Technical characteristics for an automatic identification system using time-division multiple access in the VHF maritime mobile band"*, International Telecommunications Union.

[17] S. Ghez, S. Verdú, Stuart C. Schwartz, *"Stability Proprerties of Slotted Aloha with Multipacket Reception Capability"*,IEEE transactions on automatic control, vol.33, No.7, July 1988.

[18] K.Murota, K.Hirade, *"GMSK Modulation for Digital Mobile Radio Telephony"*, IEEE transactions on communications, Vol. com-29, No. 7, July 1981.

[19] Next generation DVB-RCS standardization group. [Online]. Available: http://www.dvb.org/technology/dvbrcs.

[20] C. Morlet, A. B. Alamanac, G. Gallinaro, L. Erup, P. Takats, and A. Ginesi, *"Introduction of mobility aspects for DVB-S2/RCS broadband systems"*, IOS Space Commun., vol. 21, no. 1-2, pp. 5-17, 2007.

[21] G. Liva, *"Graph-Based Analysis and Optimization of Contention Resolution Diversity Slotted Aloha"*, IEEE Trans. Commu, vol. 59, no.2, pp. 477-487, Feb. 2011.

[22] E. Paolini, G. Liva and M: Chiani *"High Troughput Random Access via Codes on Graphs: Coded Slotted ALOHA'*, in Proc. 2011 IEEE, Int. Conf. Commu., Kyoto, Japan, Jun. 2011.

[23] K. Narayanan and H. D. Pfister, *"Iterative Collision Resolution for Slotted ALOHA: An Optimal Uncoordinated Transmission Policy"*, in Proc. 2012 7th International Symposium on Turbo Codes and Iterative Information Processing (ISTC), Gothenburg, Sweden, Aug. 2012.

[24] T. Richardson and R. Urbanke, *" Modern coding theory"*. Cambridge University Press., 2008.

[25] E. Paolini, G. Liva, and M. Chiani, *"Graph-Based Random Access for the Collision Channel without Feed-Back: Capacity Bound,"*,in Proc.2011 IEEE Global Telecommun. Conf., Houston, Texas, Dec.

[26] G. Liva, E. Paolini, M. Lentmaier, and M. Chiani *"Spatially-Coupled Random Access on Graphs"*,in Proc. IEEE Int. Symp. on Information Theory, Cambridge, MA, USA, Jul. 2012.

[27] R. Storn and K. Price, *"Differential evolution-a simple and efficient heuristic for gloabal optimization over contiuos spaces,"* J. Global Optimization, vol.11, no. 4, pp. 341-359, Dec 1997.

Acknowledgements

It has been a pleasure and an honour for me to finish my master degree here at DLR.

For first I would like to say thanks to my professors, precisely to professor Chiani and professor Paolini because they gave me the possibility to have this fantastic opportunity and because they have had trusted in me. They were periodically in contact with the supervisors at DLR and their help it has been fundamental. I hope that they will satisfied about me, for me it will mean a lot.

A second thanks not for importance, is directed to Gianluigi and Federico. Beyond their availability to accept me, they gave me the feel to be at home. I have appreciated too much their suggestions, their help and their patience with me. I have learned a lot and this is due to them. I have worked with fantastic men.

A special thanks is for Francesca. I know how much hard has been for her to stay far from me, but she has been always happy for me because she knew that I wanted to do this. I knew that she was always present, for any question or suggestion. Her presence has been very important to me, as in the previous eight years. Thanks.

Another thanks is for my 'botta di vitas' friends. Both the oldest and the youngest friends into the group are important for me. I have seen them few times during the last months but each of them knows which is the relationship with me. Their friendship has been shown also during this period, with calls and messages. Thanks to everyone of them for this.

A big thanks to my oldest university friends, especially to Vinz, Les and Marco. I hope we can find the time for continue to travel into the Europe as in these university years. You have been special colleagues.

I would like to say thanks to my sister Marta. She received me in Mu-

nich and she was always present in case of necessity. I wish to her and her boyfriend Marco the best wishes for their future.

The last thanks is for the DLR group, especially to the spanish friends. Thanks for every crazy night that we have stayed together. It is impossibile to forgive you and forgive Munich.

Iacopo